EXPERIMENTAL INVESTIGATION OF THERMAL AND RHEOLOGICAL BEHAVIOR OF HEXAGONAL BORON NITRIDE NANOFLUIDS

By

Melike Kurt

B.S, Mechanical Engineering, Istanbul Technical University, 2011

Submitted to the Institute for Graduate Studies in
Science and Engineering in partial fulfillment of
The requirements for the degree of
Master of Science

Graduate Program in Mechanical Engineering
Boğaziçi University

2014

...to the happy memories and my family

ACKNOWLEDGEMENT

First of all, I am indeed very fortunate to have Professor Ertürk as my research advisor and mentor. He is truly a smart researcher, a sincere professional, and an excellent guide. I am grateful for his inspiration and encouragement towards my academics, and personal life. I would like to mention his patience that gives me hope when I was stuck at dead ends. Secondly, I would like to express my sincere gratitude to Professor Atalık for his guidance and help during the preparation of this dissertation. And also, I should mention the support and help of Professor Atay during the preparation of this thesis. She pointed out all the small details that I easily missed out, and has been a great help for this study by providing surfactant, SDS, that we were having a hard time to find. I am really lucky to have her in my defense jury.

I would like to especially thank to my lab mate Beybin İlhan for all of her help and support at every time of need. Though words cannot express my gratitude to her, she has been a great friend above all. I wouldn't overcome the obstacles that I faced throughout this experimental study without her infinite patience and calm. Furthermore, my other lab mates; Refet Ali Yalçın, Tolga Akıner, Bahar Öner, have been a great support, thank you for the enjoyable times we spent in and out of the lab together with full of laughter.

I would also like to thank to my friends Tuğçe Göksu Utecht, Büşra Tayfur, Mehpare Atay, Mert Satır, Eylül Görmüş, Elif Saba Merç, and Ferzan Tapramaz for all the time we spent together, all the conversations we had for hours, and all the support they gave me throughout the years. Their laughter makes the life easier, when it becomes harder. Also, I would like to thank to Uğur Selçuk Büyük, for standing by me during the completion of this dissertation and convincing me to continue with my work again and again, for every time I had doubts.

My mother and father have sacrificed a lot to bring me up. My achievements have been, and will continue to be, a reaction of their love. Words of gratitude will never justify their contribution. I know they are very proud of me, and that gives me much happiness.

This thesis has been supported by The Scientific and Technological Research Council of Turkey (TUBITAK), under the grant 111M1777 of the 1001 Program.

ABSTRACT

EXPERIMENTAL INVESTIGATION OF THERMAL AND RHEOLOGICAL BEHAVIOR OF HEXAGONAL BORON NITRIDE NANOFLUIDS

In this study, thermal and rheological behavior of nanofluids prepared with hexagonal boron nitride (hBN) nanoparticles is the main interest. hBN is a ceramic material with high thermal conductivity and superior chemical stability that makes it a suitable candidate for nanofluid synthesis. Additionally, it has an orthotropic thermal conductivity which encourages study on their behavior within nanofluids. The studies that focus on hBN nanofluids are mostly limited to hBN-oil dielectric nanofluids. However, using hBN with other base fluids has also significant potential applications. This study focuses on stability, rheological and thermal behavior of hBN-water and hBN-ethylene glycol (EG) nanofluids that have not been investigated in detail. Thermal and rheological behaviors of nanofluids prepared either with pH control or surfactant addition have been investigated, and reported for different volume concentrations. All prepared nanofluids exhibit Newtonian behavior. Due to particle loading to the base fluid, viscosity increase has been observed within nanofluids as expected. Surfactant addition clearly results in higher viscosity increase and lower thermal conductivity enhancement within nanofluids comparing to ones prepared with pH control. Thermal enhancement for hBN nanofluids is found to be better than the one for Al_2O_3 nanofluids.

ÖZET

HEKZAGONAL BOR NİTRÜR NANOAKIŞKANLARININ ISIL VE REOLOJİK ÖZELLİKLERİNİN DENEYSEL OLARAK ARAŞTIRILMASI

Bu çalışmada, hekzagonal bor nitrür (hBN) nanoparçacıkları ile hazırlanmış olan nanoakışkanların ısıl ve reolojik özellikleri araştırılmıştır. hBN seramik bir malzeme olup, üstün kimyasal kararlılığı ve yüksek ısıl iletim katsayısı ile nanoakışkan hazırlamak için en iyi seçeneklerden biridir. hBN nanoparçacıkları kullanılarak yapılmış olan nanoakışkan çalışmaları genellikle hBN-yağ bazlı nanoakışkanlar olarak sınırlanmış olup, diğer baz sıvılar kullanılarak yapılacak olan çalışmaların potansiyel getirileri olduğu görülmektedir. Bu sebeple, bu çalışmada detaylı bir şekilde incelenmemiş olan hBN-su, hBN-etilen glikol (EG) ve hBN-su-etilen glikol gibi nanoakışkanlar hazırlanmış olup, bu nanoakışkanların çeşitli parçacık hacim derişimlerinde ısıl ve reolojik özellikleri araştırılmıştır. ‘ adımlı yöntem kullanılarak hazırlanmış olan bütün nanoakışkanlar Newtonyen özellik göstermektedir. Parçacık eklenmesinden kaynaklı, nanoakışkanların viskozitesinde baz sıvıya oranla bir artış beklenmektedir, ve bu çalışmada da bu artış gözlenmiştir. pH kontrolü yapılarak hazırlanmış olan nanoakışkanlara kıyasla, yüzey aktif madde kullanılması, viskozitede daha yüksek ve ısıl iletkenlikte daha düşük bir artışa sebep olmuştur. Ayrıca Al_2O_3 nanoakışkanlarına kıyasla, hBN nanoakışkanlarında daha yüksek bir ısıl iletkenlik artışı gözlenmiştir.

TABLE OF CONTENTS

LIST OF FIGURES

LIST OF TABLES

LIST OF SYMBOLS

c_p	Heat capacity of the fluid
d_{bf}	Molecular diameter of base fluid
d_p	Diameter of nanoparticles
D	Inner diameter of the pipe
g	Gravitational acceleration
h_x	Local heat transfer coefficient
h(r)	Vertical distance between cone surface and plate
i	Arbitrary measurement
k_{bf}	Thermal conductivity of base fluid
k_f	Thermal conductivity of the fluid medium
k_{nf}	Thermal conductivity of nanofluid
k_p	Thermal conductivity of particles
l	Length of the pipe
$\dot{m}$	Mass flow rate
M	Applied torque to the fluid
n	Shape factor for Hamilton and Crosser model
Nu_x	Local Nusselt number
P	Perimeter of the pipe
Pr	Prandtl number
q'	Heat per length of the wire
q"	Surface heat flux around the tube
r	Radius of the medium
r'	Radial direction in spherical coordinates
R	Radius of spherical particles
Re	Reynolds number

S_i	Uncertainty for the measurement of i
t	Function of time
T	Temperature
T_o	Initial temperature of the medium
$T_{m,i}$	Inlet mean temperature
$T_{m,o}$	Outlet mean temperature
$T_{m,x}$	Local mean temperature
$T_{s,x}$	Local surface temperature
x	Position along the pipe
v	Settling velocity
$v_{r'}$	Velocity in radial direction
v_z	Velocity in vertical direction
v_ϕ	Velocity in ϕ direction
V_f	Volume flow rate
α_f	Thermal diffusivity of fluid
ΔT	Transient temperature change
ϕ	Direction in spherical coordinates
$\dot{\gamma}$	Shear rate
φ	Volume concentration
μ_{bf}	Dynamic viscosity of base fluid
μ_{nf}	Dynamic viscosity of nanofluid
π	Pi number
θ	Direction in spherical coordinates
θ_o	Cone angle
ρ	Density
ρ_p	Density of particle
ρ_{bf}	Density of base fluid
σ	Shear stress tensor

ω	Rotational velocity

LIST OF ACRONYMS / ABBREVIATIONS

BN	Boron nitride
BNNS	Boron nitride nanosphere
BNNT	Boron nitride nanotube
CNT	Carbon nanotubes
CTAB	Cetyltrimethylammonium bromide
DI	De-ionized
DLS	Dynamic light scattering
DTAB	Dodecyl trimethylammonium bromide
EG	Ethylene glycol
ESEM	Environmental scanning electron microscopy
GA	Gum Arabic
hBN	Hexagonal boron nitride
HCTAB	Hekzadecyl trimethylammoniumbromide
IEP	Isoelectric point
MO	Mineral oil
PAO	Polyalpha olefin oil
PDDA	Polydiallyldimethylammonium chloride
PG	Propylene glycol
PVD	Physical vapor deposition
PVP	Polyvinyl pyrrolidone
SDBS	Sodium dodecyl benzene sulfonate
SDS	Sodium dodecyl sulfate
SEM	Scanning electron microscopy
SOCT	Sodium octanade
STEM	Scanning transmission electron microscopy
TEM	Transmission electron microscopy
THW	Transient hot wire
TNT	Titanate nanotubes

UV-Vis	Ultraviolet–visible spectroscopy
VEROS	Vacuum evaporation onto a running oil substrate

1. INTRODUCTION

1.1. Problem Overview

In many engineering applications, improved heat transfer is critical either to improve system efficiency or for safe/reliable operation of systems. There have been numerous research efforts on heat transfer enhancement in wide range of applications, from energy systems to vehicles or opto/electronic thermal management. One of the main topics is to improve heat transfer through the use of engineered materials such as heat transfer fluids. By introducing small particles to a base fluid, improved thermal properties can be obtained with respect to base fluid. In order to prevent clogging within the channels and stability issues within these engineered heat transfer fluids, these small particles are chosen to be nanometer sized particles. These nanoparticle based colloidal suspensions are named as "nanofluids" (Choi, 1995). Since their introduction, nanofluids are often regarded as next generation heat transfer fluids, and their use has become a popular topic of debate that has aroused the attention of heat transfer research community.

The main problems in the implementation of nanofluids into the engineering systems are the stability issues and viscosity increase that often surpasses thermal enhancement. The first and the most important problem considered in regards to the use of nanofluids is their stability in the long term use. The preparation recipe of nanofluids should be carefully predetermined because nanoparticles tend to agglomerate due to their high surface energy, and these agglomerates lead to sedimentation, which indicates unstable colloidal suspensions. Second drawback in the nanofluid use is the increase in overall viscosity that might surpass the improvement obtained in thermal enhancement. In the engineering applications, increased viscosity leads to higher pumping power or slower flow. Since slower flow deteriorates the heat transfer performance, preparation of a nanofluid with lower viscosity, higher thermal enhancement and better stability is the main challenges in the commercialization of nanofluids.

1.2. Literature Survey

Nanofluids are colloidal suspensions that are prepared by introducing solid nanoparticles of approximately less than 100 nm size into a base fluid. There have been extensive research efforts to explore thermal properties and convection heat transfer behavior of nanofluids, since the term "nanofluid" was introduced by Choi (1995). The nanofluids have been declared as "next generation heat transfer fluids", as even for very low particle concentrations a dramatic enhancement in thermal conductivity is observed. As a result, they are considered to be utilized in many thermal applications such as energy systems or thermal management applications. As the mechanism behind the dramatic thermal enhancement is not clear, and due to concerns about their stability, commercialization of nanofluids is still a popular topic of debate.

In order to prepare nanofluids, the first challenge that the researchers confront is to maintain stability of nanoparticles within the fluid for a long time period. The settling velocity of a particle within a base fluid can be explained by Stokes formula (Ghadimi *et al.*, 2011).

$$v = \frac{2R^2}{9\mu_{bf}} g(\rho_p - \rho_{bf}) \tag{1.1}$$

In Equation 1.1, v is the settling velocity of particles within the fluid; R, radius of spherical particles; μ_{bf}, dynamic viscosity of the base fluid; ρ_p and ρ_{bf}, density of particles and base fluid; and g, the gravitational acceleration. From this formula it can be asserted that the stability of particles within the fluid can be enabled by the balance of gravitational, buoyancy and viscous forces. According to Equation 1.1, the following measures can be taken in order to reduce settling velocity and to improve stability of particles within the base fluid: reducing particle size, increasing base fluid's dynamic

viscosity, and minimizing the difference between density of particles and the base fluid $(\rho_p - \rho_{bf})$. In the case of nanometer sized particles, settling velocity can even be zeroed with the effect of Brownian motion that is defined as the random motion of particles suspended into a fluid. However, the decrease in the particle size causes the increase in the surface attraction forces between nanoparticles, and consequently it encourages nanoparticles to agglomerate and settle down. In order to provide stability within the nanofluid, the agglomeration of nanoparticles must be prevented.

1.2.1. Nanofluid Preparation and Stability Improvement Methods

There are two nanofluid preparation methods; one step method and two step method. In the one step method, manufacturing of nanoparticles and preparation of nanofluid are carried out as a single process. Physical vapor deposition (PVD), and vacuum evaporation onto a running oil substrate (VEROS) are used in this method to prepare nanoparticles and nanofluids instantly. The advantage of this method is that the agglomeration and stability problems are minimized due to the concurrent preparation of nanoparticles and nanofluid. However, this method is harder to implement for industrial production as it is harder to implement it for mass production. Considering the potential industrial applications, one step method is not preferred to prepare nanofluids in this study.

The most common method of nanofluid preparation in the literature is the two step method which allows easier implementation and mass production in industrial processes (Ghadimi *et al.*, 2011). In this method, dry nanoparticles are introduced into the base fluid in low volume fractions. However, the high surface energy of nanoparticles results in agglomeration and clustering, and that is easily distinguishable within the nanofluid. Because of that, stability becomes an important problem. In order to prevent this problem, additional techniques must be implemented as stability improvement methods such as ultrasonication, pH control, and surfactant addition.

1.2.1.1. Ultrasonication. When piezoelectric materials such as quartz and sodium potassium tartarate are exposed to strain, electric current is produced. On the contrary, if electric current is applied to these materials, they will expand or contract. By using piezoelectric characteristic of these materials, equipments which are vibrating at ultrasonic frequencies can be designed.

When an ultrasonically vibrating probe is placed into a fluid, low pressure is generated around the ultrasonic probe and the fluid begin to move. If the frequency of ultrasonicationis increased sufficiently enough, this movement stops and fluid molecules begin to vibrate which leads to formation of vacuum bubbles and microscobic shock waves within the fluid. These shock waves fade within microseconds, but it releases sufficient amount of energy to reduce the size of nanoparticle agglomerates within the fluid (Perez *et al.*, 2004).

In two step method, ultrasonication is a technique that is widely used to provide homogeneous colloidal dispersions. If the dispersion is not mixed for a sufficient time to reduce the nanoparticle agglomerate size, instability within the nanofluid is unavoidable. On the other hand, if the dispersion is vibrated too long, fragmentized nanoparticles can re-agglomerate due to the effect of high surface energy. Thus, an optimal sonication time needs to be determined to provide optimal agglomeration size and as a result stability within the nanofluid for every nanoparticle, base fluid type, and particle volume concentration (Ghadimi *et al.*, 2011).

1.2.1.2. pH Control. The stability of nanofluids is related to their electrokinetic properties. It is possible to prepare more stable nanofluids by increasing the surface electric charge density of nanoparticles (Chou *et al.*, 2005; Wang *et al.*, 2009; Wei *et al.*, 2009; Zhu *et al.*, 2009). The isoelectric point (IEP) is the pH that overall electric charge of ions within a fluid is zero which means its zeta potential is zero. If the zeta potential of the fluid is not high enough, or attraction forces will overcome the repulsive forces between

nanoparticles and they will agglomerate. On the contrary, repulsive forces between nanoparticles will be dominant with increasing zeta potential. Thus, it can be inferred from these statements that the stability of the nanofluid increases when the nanofluid's electric charges diverges from IEP (Chou *et al.*, 2005; Huang *et al.*, 2009; Lee *et al.*, 2006; Wei *et al.*, 2009). Therefore, pH control is another method to increase stability of nanoparticles within the nanofluids.

Zeta potential can be increased by changing the pH in order to provide stability (Chou *et al.*, 2005; Lee *et al.*, 2006; Wang *et al.*, 2009; Wei *et al.*, 2009; Witharana *et al.*, 2012; Yang *et al.*, 2010; Zhu *et al.*, 2009; Zhu *et al.*, 2010). Optimal pH values should be determined for different base fluid-nanoparticle suspensions, depending on the electrokinetic properties. In this study, pH control is one of techniques that are employed to accommodate stable colloidal dispersions.

1.2.1.3. Surfactant Addition. Surfactant addition is one of the most common techniques to mitigate agglomeration of nanoparticles. It is possible to change hydrophobic behavior of nanoparticles and nanotubes into hydrophilic by using surfactant additives, and with the effect of nanoparticles' electrokinetic zeta potential, repulsive forces can be increased within liquid medium (Huang *et al.*, 2009; Hwang *et al.*, 2007). The amount of surfactant added to suspension is important. Stability can be obtained with the right amount of surfactant that encourages repulsive forces to become dominant against van der Waals forces which is the indication of attraction forces between nanoparticles. However, surplus surfactant can lead to a decrease in thermal properties of nanofluids (Ghadimi *et al.*, 2011).

There are numerious type of surfactant used in the nanofluid literature. Sodium dodecyl sulfate (SDS), sodium dodecyl benzene sulfonate (SDBS), salt and oleic acid, cetyltrimethylammonium bromide (CTAB), dodecyl trimethylammonium bromide (DTAB), sodium octanade (SOCT), hekzadecyl trimethylammoniumbromide (HCTAB), and polyvinyl pyrrolidone (PVP) are the most common surfactants used in nanofluids (Wu

et al., 2009). Gum Arabic (GA) is another surfactant that has an organic structure and is generally used for carbon nanotubes (CNT). In the literature, there are several studies where GA is used to stabilize CNTs (Amrollahi *et al.*, 2009; Lee *et al.*, 2010; Rashmi *et al.*, 2010; Walwekar *et al.*, 2012). Moreover, in the study of Pang *et al.* (2013) GA with the addition of salt (NaCl) is used to stabilize Al_2O_3 nanofluids.

Since surfactant addition affects interactions between fluid and solid molecules, it may lead to a decrease in the thermal properties. In this study, GA and SDS are used as surfactants for hBN nanofluids.

These additional techniques, ultrasonication, pH control, and surfactant addition, are necessary to prevent rapid agglomeration and sedimentation of nanoparticles, to obtain stability within the nanofluid. Just one of these methods or a combination of them can be used during the preparation of nanofluids in order to acquire stable dispersions. In Table 1.1, stability improvement methods that are used in some of the studies within the literature are summarized. In the experimental study of Patel *et al.* (2005), 11 nm sized alumina nanoparticles with 0.8% volume fraction were stabilized within water as a base fluid by sonicating the suspension for 6 hours. Das *et al.* (2003) reported that after sonicating Al_2O_3 and CuO nanofluids for 12 hours, no sedimentation was observed within 12 hours for 1, 2, 3, 4% volume concentrations and after 12 hours, minor sedimentation was observed in 3 and 4% volume concentrations. Due to the nature of nanoparticles or preparation method, only using sonication may not be sufficient to enable stability within the nanofluid. Thus, a combination of treatments might be required. Huang *et al.* (2009) used ultrasonication, pH control and surfactant additives all at once to obtain stable Al_2O_3/Cu-water suspensions. In this study, the effective particle size within the nanofluid was successively reduced and stability of nanofluids was improved by using SDBS dispersant and optimizing the pH. In the study of Chen *et al.* (2009), no dispersant/surfactant was used during the preparation in order to avoid complications in the results of thermal conductivity experiments. TiO_2 nanoparticles and titanate nanotubes (TNT) were dispersed into both EG and de-ionized (DI) water base fluids and they were

Table 1.1. Summary of the stability improvement methods that are used in nanofluid studies.

Study	Nanofluid	Sonication	pH Control	Additives
Das *et al.* (2003)	Al_2O_3 /CuO-water	×	–	–
Patel *et al.* (2005)	Al_2O_3-water	×	–	–
Huang *et al.* (2009)	Al_2O_3 / Cu – water	×	×	SDBS
Chen *et al.* (2009)	TiO_2 / TNT - water / EG	×	×	–
Nasiri *et al.* (2011)	CNTs - water	×	–	SDS
Zhi *et al.* (2011)	BN nanotubes and nanospheres - water	×	×	PDDA
Fedele *et al.* (2011)	CNTs / TiO_2 - water	×	–	SDS
Pang *et al.* (2013)	Al_2O_3 - water	×	×	GA

found to be stable for at least 1 month by using sonication, magnetic stirring and pH control during the preparation process.

1.2.2. Stability Inspection Methods

Stability is the key feature in the nanofluid preparation procedure; therefore it is important to determine stability. In order to determine the level of stability, different methods are used. There are seven different methods used to inspect stability of nanofluids in the literature.

1.2.2.1. UV – Vis Spectrophotometer. Ultraviolet–visible spectroscopy (UV-Vis) refers to absorption or reflectance spectroscopy in the ultraviolet-visible wavelengths. UV-Vis measurements have been used to quantitatively characterize colloidal stability of the dispersions.

A UV-Vis spectrophotometer exploits the fact that the light intensity attenuates by absorption and scattering as light passes through a fluid. In this method, at first the maximum absorbtance of the dispersed nanoparticles at very dilute suspension should be found by scanning. The next step is to obtain a linear relation between volume concentration of the suspension and absorbtance. By preparing a standard to fit the linear relation between volume concentration and absorbtance for at least three different concentrations (0.01-0.03%), relative stability analysis can be employed for the nanofluids prepared with desired volume concentration in time. This method is the application of Beer-Lambert law and is used to determine the stability level of the nanoparticle suspensions in several studies (Hwang *et al.,* 2007; Kim *et al.,* 2007; Lee *et al.,* 2009). One of the most striking features of this method is its applicability for all base fluids, whereas for other stability analysis methods such as zeta potential measurements have restrictions for the viscosity of the host fluid.

1.2.2.2. Zeta Potential Test. Measuring zeta potential of the synthesized nanofluid is one of the most used methods in stability inspection. The increase in the zeta potential indicates an increase in the repulsive forces between nanoparticles within the nanofluid as stated before (Chou *et al.,* 2005; Lee *et al.,* 2006; Wang *et al.,* 2009; Wei *et al.,* 2009; Witharana *et al.,* 2012; Yang *et al.,* 2010; Zhu *et al.,* 2009; Zhu *et al.,* 2010). Thus, high zeta potential values discourage the formation of agglomerates, and eventually, lead to good stability. Incipient stability can be obtained at ±10 - ±30 mV zeta potential values, whereas the zeta potential values between ±30 - ±40 mV implies moderate stability, ±40 - ±60 mV good stability, and the zeta potential values more than ±60 mV points out excellent stability. One of the drawbacks of this method is that it cannot be employed for the suspensions with high viscosity.

Zeta potential measurements are performed by using a probe to create electric field within a vessel. This electric field enables nanoparticles to accelerate between two sides and by using laser-doppler anemometry, the velocity of these particles is determined. As a result, zeta potential value of nanoparticles within the liquid media can be calculated by

relating the velocity of nanoparticles and electrical conductance of the liquid medium to zeta potential. Dilution of the prepared nanofluids should be employed as it is used in the several other nanofluid studies such as the study of Lai (2010) and Wu *et al.* (2009).

1.2.2.3. DLS Method. This method is used to investigate polymer molecules and colloidal particles within the suspensions, therefore it can be employed for nanofluids as well. In this method, the intensity of the scattered light is related to the effective particle size. Since the method relies on the single scattering approximation the tested nanofluid should be diluted if necessary. DLS method is one of the most used methods, employed to acquire the level of agglomeration by measuring the mean aggregate size (Colla *et al.*, 2012; Fedele *et al.*, 2011; Wang *et al.*, 2009) within the suspension. While smaller mean aggregate size refers to improved dispersions, larger mean aggregate size indicates existence of significant agglomerates.

1.2.2.4. TEM (Transmission Electron Microscopy) and SEM (Scanning Electron Microscopy). TEM is a microscopy technique that uses electron beams which is transmitted through an ultra-thin sample. Interaction of electron beams with the sample is used to form an image, and by magnifying or focusing onto an imaging device, or detecting by a sensor, TEM image can be obtained. In SEM, similar to TEM, test sample is exposed to an electron beam which generally follows a rectangular scan pattern that is called raster scan pattern to capture an image. The information provided from the scattered electrons is about sample's topography and composition. The main difference between TEM and SEM is that TEM uses transmitted electrons whereas SEM uses scattered electrons. Furthermore, SEM provides information only about sample's morphology while TEM can show many characteristics of the sample such as morphology, crystallization, stress or even magnetic domains.

Agglomeration size and shape of nanoparticles within the nanofluid which might enable the abnormal heat transfer capability of nanofluids are important factors to explain

thermal enhancement mechanisms within the nanofluid, (Li *et al.*, 2011; Taha-Tijerina *et al.*, 2012). TEM and SEM imaging can be used, since it is useful to observe the nanoparticles' colloidal structure within the nanofluids. However, as imaging of particles within a nanofluid sample is not possible, images of dried nanoparticles are captured. Images taken for dried nanofluid samples can be helpful to designate particle size and shape (Fedele *et al.*, 2011; Hong *et al.*, 2012; Wang *et al.*, 2009; Witharana *et al.*, 2012; Xuan *et al.*, 2000).

1.2.2.5. Qualitative Imaging. A primary method to observe sedimentation qualitatively within nanofluids is imaging (Wang *et al.*, 2009; Wei *et al.*, 2009; Zhu *et al.*, 2009; Witharana *et al.*, 2012). After preparation, a volume of the suspension will put aside to capture its images at a defined time period. As local volume concentration of particles affect the colour of suspension, comparing these photos of nano suspensions, sedimentation of suspension can be clearly observed. Qualitative imaging is one of the most common methods because of its easy implementation. However, it is a qualitative method so it gives no quantitative information about the stability level of the nanoparticle suspensions.

1.2.2.6. Sedimentation Balance Method. The stability of the nanoparticle suspension can also be measured by using another method called sedimentation balance. In this method, a balance is placed into the newly prepared nanofluid to measure the amount of sedimentation, and in time, amount of sedimentation is determined. By calculating the amount of sedimentation, rate of sedimentation in time and volume fraction of the supernatant nanofluid can be determined. This method is used in the study of Zhu *et al.* (2007) in order to determine the stability level of suspensions of graphite nanoparticles.

1.2.2.7. Stability Detection By Measuring Thermal Conductivity. Another method to determine the colloidal stability level of nanoparticle suspensions is to relate thermal conductivity and the sedimentation level of nanofluids. A wide range of volume

concentrated nanofluids should be tested to obtain the sedimentation level – thermal conductivity relation. This method has found a few uses in the nanofluid literature in which 3-ω method is employed to measure thermal conductivity (Oh *et al.*, 2008; Wang and Sen, 2009).

1.2.3. Thermal Conductivity Enhancement of Nanofluids

In the solvent media, nanoparticles have an abnormal effect on thermophysical properties. The property that has aroused the attention of nanofluid research community the most is thermal conductivity. Currently there is no agreed theory for predicting the anomalous behavior of thermal conductivity of nanofluids. According to experimental results of many researchers, it is clear that the thermal conductivity of nanofluids depends on several physical parameters such as thermal conductivities of the base fluid and nanoparticles, volume fraction of particle loading, surface area of the nanoparticles within the nanofluid, the shape of nanoparticles, and the temperature.

Numerous theoretical studies have been conducted to predict the thermal conductivity of particle-fluid mixtures. According to Maxwell's effective medium theory (Maxwell, 1881), dispersion of spherical solid particles within the liquid media is expected to have an effective thermal conductivity of,

$$\frac{k_{nf}}{k_{bf}} = \frac{k_p + 2k_{bf} + 2\varphi(k_p - k_{bf})}{k_p + 2k_{bf} - \varphi(k_p - k_{bf})} \tag{1.2}$$

where k_{nf} is the effective thermal conductivity of nanofluids, k_{bf} is the thermal conductivity of base fluid, k_p is the thermal conductivity of particle, and φ is the volume concentration of particles within the liquid media.

Another study about conductivity of solid-fluid mixtures containing spherical particles was proposed by Bruggeman (1935). According to Bruggeman's model effective thermal conductivity of the solid-fluid mixture can be predicted as,

$$\varphi\left(\frac{k_p - k_{nf}}{k_p + 2k_{nf}}\right) + (1-\varphi)\left(\frac{k_{bf} - k_{nf}}{k_{bf} + 2k_{nf}}\right) = 0 \tag{1.3}$$

Bruggeman's model has no limitations for the particle concentration within the fluid. For low volume concentrations it gives almost the same results as the Maxwell model. However, for higher volume concentrations Bruggeman's model matches well with the experimental data where Maxwell model fails (Choi, 1995).

Hamilton and Crosser (1962) proposed another model for solid-fluid mixture with non-spherical particles. In this model a shape factor, n, is introduced, and the thermal conductivity ratio of solid fluid mixtures where the ratio of thermal conductivity of solid and fluid phases larger than 100 ($k_p/k_{bf} \rangle 100$) is given as,

$$\frac{k_{nf}}{k_{bf}} = \frac{k_p + (n-1)k_{bf} - (n-1)(k_{bf} - k_p)\varphi}{k_p + (n-1)k_{bf} + (k_{bf} - k_p)\varphi} \tag{1.4}$$

By comparing Equation 1.2 and 1.4, the one can see that Maxwell's model is a special case of Hamilton and Crosser's model in which the sphericity equals to 1 ($n = 1$).

These classical models are the derivations of continuum formulations, assuming diffusive heat transport in both solid and liquid phases, and they relate solid-fluid mixtures' thermal conductivity to thermal conductivity of solid and liquid phases, volume fraction,

and shape of solid particles. They all fail to predict large enhancement of thermal conductivity of nanofluids by neglecting several other mechanisms. Some of the researchers stated that the thermal conductivity enhancement is beyond the predictions of Equation 1.2 and the dependence on particle volume concentration is nonlinear (Chopkar *et al.*, 2006; Eastman *et al.*, 2001; Hong *et al.*, 2005; Li *et al.*, 2000; Kang *et al.*, 2006; Shaikh *et al.*, 2007). It is also observed that the particle size and shape (Chen *et al.*, 2008; Chon *et al.*, 2005; Chopkar *et al.*, 2006; Hong *et al.*, 2006; Kim *et al.*, 2007; Li *et al.*, 2007; Murshed *et al.*, 2005; Shima *et al.*, 2009; Xie *et al.*, 2002), and the temperature of the nanofluid (Chon *et al.*, 2005; Das *et al.*, 2003; Li *et al.*, 2006; Wen *et al.*, 2004) have a significant effect on the enhancement.

There are several hypotheses that explains these deviations from predictions by effective medium theories. Brownian motion of nanoparticles within fluid that creates microconvection effect, causes an increase in energy transfer (Jang *et al.*, 2004; Prasher *et al.*, 2005). According to another explanation the form of the agglomerations of nanoparticles within the nanofluid creates paths for energy transport due to percolation (Eapen *et al.*, 2007; Keblinski *et al.*, 2002; Prasher *et al.*, 2006). The order of the base fluid molecules around nanoparticles induces the effect of nanoparticle loading and by increasing the effective volume concentration, base fluid molecules and nanoparticles form a highly-ordered high thermal conductivity layer that is referred as nanolayer (Eapen *et al.*, 2007a; Eapen *et al.*, 2007b; Keblinski *et al.*, 2002). On the other hand, in a benchmark study of Buongiorno *et al.* (2009) conducted with different kinds of nanofluids, it was asserted that the thermal conductivity data taken from several types of nanofluids is perfectly correspondent with the classic effective medium theory. Besides, it was denoted that the thermal conductivity enhancement increased with the particle loading, particle aspect ratio, and decreasing base fluid thermal conductivity.

Furthermore, there are some experimental correlations and models for thermal conductivity of nanofluids which are commonly used in the nanofluid literature. In the study of Chon *et al.* (2005), an experimental correlation for Al_2O_3-water nanofluids as a

function of nanoparticle size is proposed by using the measured thermal conductivity data. The correlation is represented as,

$$\frac{k_{nf}}{k_{bf}} = 1 + 64.7\varphi^{0.7460}\left(\frac{d_{bf}}{d_p}\right)^{0.3690}\left(\frac{k_p}{k_{bf}}\right)^{0.7476} Pr^{0.9955}\, Re^{1.2321} \tag{1.5}$$

where d_{bf} is molecular diameter of base fluid, d_p is diameter of nanoparticles, Pr is Prandtl number, and Re is Reynolds number. Yu and Choi (2003) derived a renovated Hamilton - Crosser model which can be expressed as,

$$\frac{k_{nf}}{k_{bf}} = 1 + \frac{n\varphi A}{1-\varphi A}; \quad A = \frac{1}{3}\sum_{j=a,b,c}\frac{k_{pj}-k_{bf}}{k_{pj}+(n-1)k_{bf}} \tag{1.6}$$

In the study of Mintsa *et al.* (2009), an experimental correlation for thermal conductivity of Al_2O_3-water nanofluids as a function of particle volume concentration is obtained as,

$$\frac{k_{nf}}{k_{bf}} = 1.74\varphi + 0.99 \tag{1.7}$$

Thermal conductivity enhancement data taken from the several studies in the literature for 40-50 nm sized Al_2O_3 nanofluids is presented in Figure 1.1a and 1.1b. According to Figure 1.1a, for lower volume concentrations (0-5%) the predictions of models correspond well with the given experimental data whereas only the model proposed by Chon *et al.* (2005) matches adequately with the experimental data for higher volume concentrations as it can be clearly seen from Figure 1.1b.

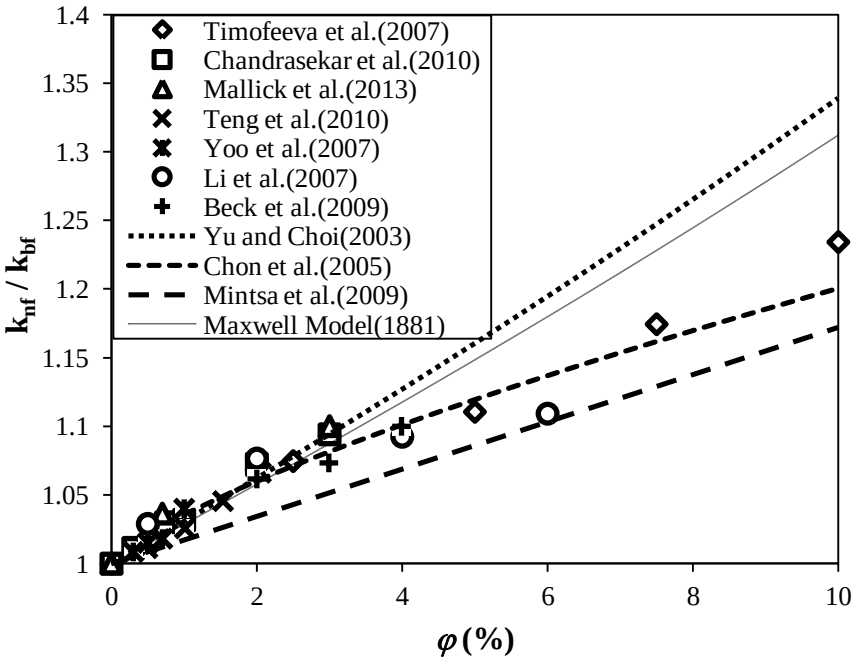

(a)

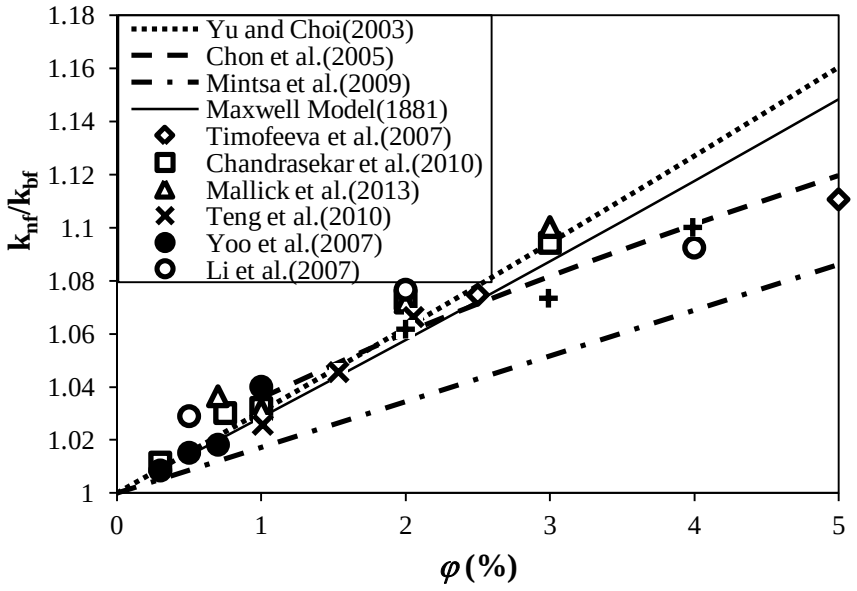

(b)

Figure 1.1. Thermal conductivity ratio of water based nanofluids containing Al_2O_3 particles of 40-50 nm changing with the volume concentration in the literature, for volume concentrations of 0-10% (a) and 0-5% (b).

1.2.4. Thermal Conductivity Measurement Methods

Thermal conductivity can be measured by a number of different methods. Depending on the thermal properties and the medium temperature, each method can be applied for a limited range of materials. Thermal conductivity measurement methods can be classified as; steady state and transient methods.

1.2.4.1. Steady State Methods. In the steady state methods, thermal conductivity measurement is performed when the measured temperature of the material does not change with time (steady state condition). Thermal conductivity of the medium is calculated by the measured temperature difference and the applied heat flux through the surface. Time independency makes this method relatively easier. However, it is not easy to satisfy the requirements of the method in practical test setups which can be described as a disadvantage. Steady state methods can be classified as, horizontal flat plate method, vertical coaxial cylinder method, steady state hot wire method, concentric cylinders method, and absolute and relative methods.

1.2.4.2. Transient Methods. Temperature variation along time at an arbitrary point is measured to estimate thermal conductivity. In steady state methods the system and the signal must reach a steady state, whereas in transient methods this signal can vary in time. Since there is no need to wait until system reaches steady state, the measurement time is shorter. However, the analysis of data is more complicated than for steady state methods. Transient thermal conductivity measurement methods can be classified as, continuous line source (transient hot wire - THW) method, transient plane source method, laser flash method, and 3-ω method.

In this study, thermal conductivity measurements are carried out by Decagon KD2Pro thermal conductivity sensor which uses transient hot wire (THW) method.

Thermal conductivity measurement with transient hot wire method is explained in detail in the next chapter.

1.2.5. Rheological Behavior of Nanofluids

It is well known that the addition of nanoparticles into a fluid can substantially change its rheological properties. The fact that nanofluids are considered as an alternative for present heat transfer fluids makes their rheological behavior more crucial. It is obvious that besides thermal conductivity, viscosity is an important factor on overall heat transfer performance of a heat transfer fluid. With altered viscosity, a heat transfer fluid might demand more pumping power, which may surpass the benefit from enhanced thermal conductivity of the nanofluid.

Einstein (1905) was the first to formulate effective viscosity of solid-fluid mixture containing spherical particles by using hydrodynamic equations. According to Einstein's theory, the effective viscosity of solid-fluid mixture is linearly dependent only on volumetric particle concentration, and it can be defined as,

$$\mu_{\mathrm{nf}} = (1 + 2.5\varphi)\mu_{\mathrm{bf}} \tag{1.8}$$

where μ_{nf} is the viscosity of the solid-liquid mixture, and μ_{bf} is the viscosity of base fluid. Similar to Einstein's formula, Lundgren (1972) is proposed another model as,

$$\mu_{\mathrm{nf}} = (1 + 2.5\varphi + 6.25\varphi^2)\mu_{\mathrm{bf}} \tag{1.9}$$

Furthermore, Batchelor (1977) introduces a similar model as well as it is presented in Equation 1.10.

$$\mu_{nf} = (1 + 2.5\varphi + 6.5\varphi^2)\mu_{bf} \tag{1.10}$$

A different model is proposed by Brinkman (1947) which gives similar results as well, represents effective viscosity as the power of the volume concentration.

$$\mu_{nf} = \left(\frac{1}{1-\varphi^{2.5}}\right)\mu_{bf} \tag{1.11}$$

These effective medium models are derived for 0-2% particle volume concentrations. All these models are given similar results for low volume concentrations (0-10%).

There have been several studies on the rheological behavior of nanofluids (Buongiorno *et al.*, 2009; Chen *et al.*, 2009; Venerus *et al.*, 2010; Prasher *et al.*, 2006). According to Chen *et al.* (2009), nanofluids prepared by dispersing TiO_2 nanoparticles into EG were found to exhibit Newtonian behavior, whereas water - TiO_2, water - TNT, and EG - TNT nanofluids show non-Newtonian behavior. Dependency of viscosity on particle loading was found to be stronger than the one predicted by Einstein or Batchelor's model for all nanofluids. A benchmark study that is conducted by Venerus *et al.* (2010) reports identical behavior; viscosity of nanofluids with both spherical and rod-shaped particles suspended into water and polyalpha olefin oil (PAO), showed a stronger dependency on volume concentration than the one predicted by dilute suspension theory. In this study, five of the seven nanofluids tested showed Newtonian behavior as other two showed shear thickening behavior. Furthermore, in the study of Prasher *et al.* (2006), alumina particles with three different sizes (27, 40, 50 nm) were introduced into propylene glycol (PG) and the

viscosity measurements of these nanofluids for three different volume concentration (0.5, 2, 3%) all showed Newtonian behavior. The particle loading dependency of viscosity was again found to be much higher than the one predicted by Einstein - Batchelor theory. These three rheological studies indicate that strong dependency on particle loading is due to the microstructural form of the nanoparticles (agglomerations) within the nanofluids. A brief summary of rheological studies about nanofluids is given in Table 1.2. Although, there are exceptions, it can be interpreted that the rheological behavior of nanofluids, whether they are Newtonian or non-Newtonian, mostly depends on the base fluid and the amount of particle loading. In Figure 1.2a and b, viscosity increase data with the increase in volume concentration of Al_2O_3 nanofluids is presented. Data series taken from experimental studies are compared with Einstein's formula, Lundgren and Batchelor's formula, and the polynomial fit proposed by Maiga *et al.* (2004) for 0-10% and 0-5% volume concentrations respectively. As it can be clearly observed from Figure 1.2a, Einstein's, and Lundgren and Batchelor's formula generally underestimate experimental data whereas the polynomial fit of Maiga *et al.* (2004) corresponds well with the given ex-

Table 1.2. A brief summary of rheological studies about nanofluids in the literature.

Study	Nanofluid	Behavior
Chen *et al.* (2009)	TiO_2 - EG	Newtonian
	TiO_2 - water	non-Newtonian
	TNT - EG	non-Newtonian
	TiO_2 - water	non-Newtonian
Venerus *et al.* (2010)	Al_2O_3-water (rod)	Newtonian
	Al_2O_3-PAO+surf. (sphere)	Newtonian
	Al_2O_3-PAO+surf. (sphere) 1% vol.	Newtonian
	Al_2O_3-PAO+surf. (rod) 1% vol.	Newtonian
	Al_2O_3-PAO+surf. (rod) 3% vol.	non-Newtonian
	SiO_2-water+stab. (sphere) 32% vol.	non-Newtonian
	$Mn_{1/2}Zn_{1/2}Fe_2O_3$-water+stab. (sphere) 0.17% vol.	Newtonian
Prasher *et al.* (2006)	Al_2O_3 - PG	Newtonian
Sleiti *et al.* (2011)	hBN-PAO	Newtonian
Tijerina *et al.* (2012)	hBN fillers - MO	Newtonian

perimental data series. From Figure 1.2b, it can be stated that experimental data series scatter around Maiga *et al.* (2004) other than data taken from the study of Liu and Yu (2011) which is in a perfect agreement with Einstein's, and Lundgren and Batchelor's formula.

1.2.6. Viscosity Measurement Methods

A viscometer is an instrument used to measure viscosity of a fluid. In the viscosity measurement devices, either fluid remains stable and an object moves or the object remains stable and the fluid passes through it. Relative motion of the fluid and the surface creates a drag which is the measure of viscosity. The Reynolds number within the fluid flow should be sufficiently low for there to be laminar flow. Viscometers can be classified as, falling piston viscometer, oscillating piston viscometer, vibrational viscometers, and rotational viscometers.

In this study a rotational viscometer, Brookfield DV-III Ultra cone-plate rheometer, is utilized to investigate rheological behaviors of nanofluids. By changing the applied torque and as a result shear rate within a limited range, rheological behaviors of nanofluids are determined. The measurement methodology of a cone-plate rheometer is explained in detail in the second chapter of this study.

1.2.7. Boron Nitride

Boron nitride is a ceramic material which is structured similarly to carbon lattice, thus exists in several crystalline forms. hBN is the most stable and the softest of all forms. Therefore, it is used as an additive to lubricants and cosmetic products. Its high thermal conductivity and superior chemical stability make it a candidate material for nanofluids.

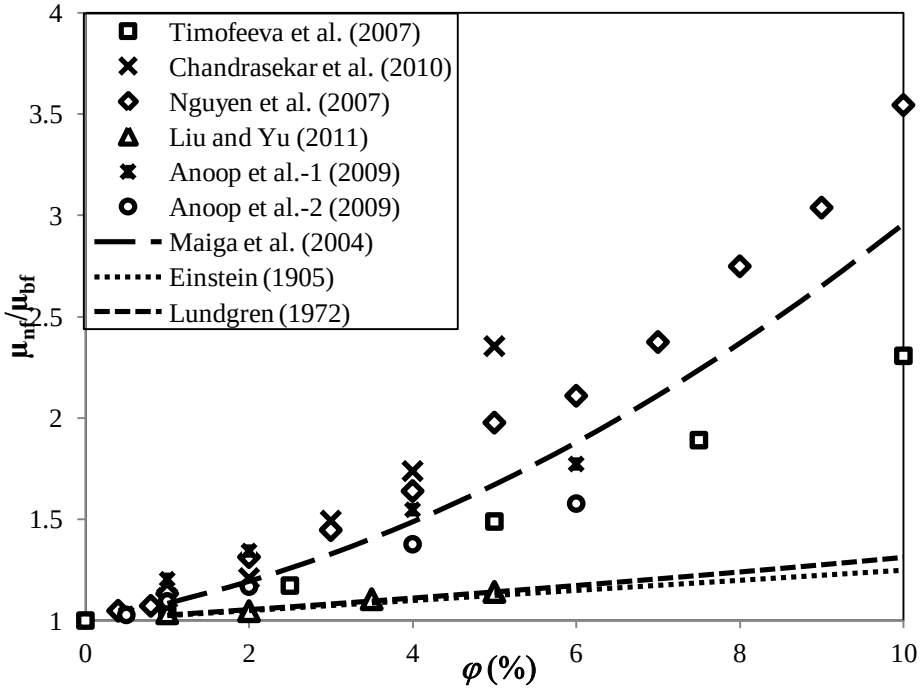

(a)

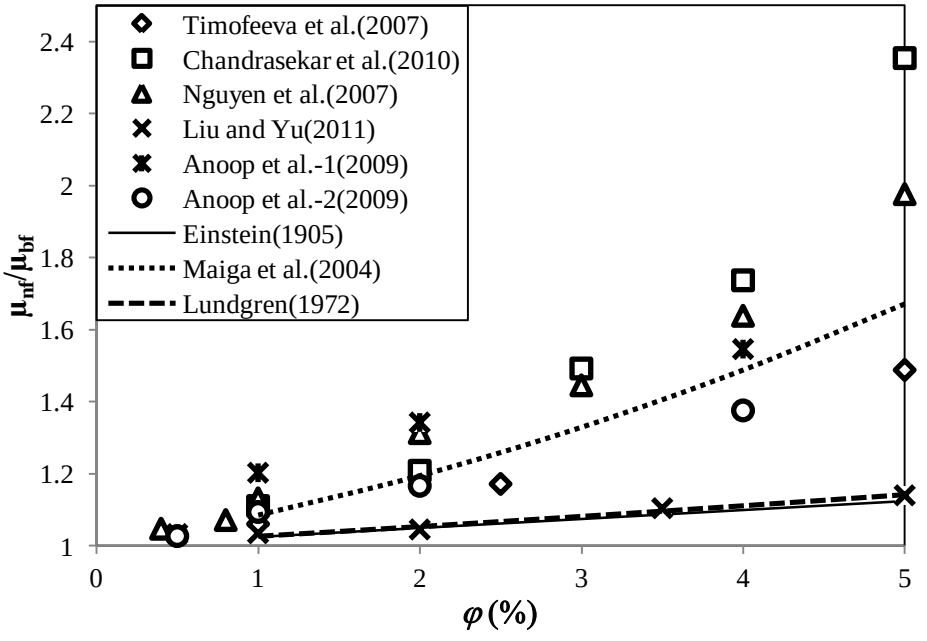

(b)

Figure 1.2. Viscosity ratio of water based nanofluids containing Al_2O_3 particles of 40-50 nm sized changing with the volume concentration in the literature, for 0-10% (a) and 0-5% (b).

There are a few studies about nanofluids of hBN nanofillers and nanoparticles in the literature (Li *et al.*, 2011; Sleiti *et al.*, 2011; Taha-Tijerina *et al.*, 2012; Zhi *et al.*, 2011).

In the experimental study of Taha-Tijerina *et al.* (2012), two dimensional hBN nano-fillers were introduced into a carrier fluid, mineral oil (MO), and thermal conductivity experiments were conducted. It was seen that at higher concentrations, the increase in thermal conductivity was not following Maxwell's theory. This behavior is attributed to percolation mechanism within the nanofluid. Moreover, strong dependency of thermal conductivity on temperature was ascribed to the increase in Brownian motion, thus reveals that the mechanism behind this thermal enhancement is not only percolation but also Brownian motion dependent. Li *et al.* (2011), reported that the thermal conductivity enhancement in 140 nm sized boron nitride (BN) – EG nanofluids is higher than the one prepared with 70 nm BN particles. This behavior was assigned to the difference in specific surface area and aspect ratio of different sized BN particles. However, the latent structures of these BN materials are not specified. If the BN particles with 140 nm and 70 nm have latent structures of cubic and hexagonal respectively, nanofluids synthesized with 140 nm cubic BN will be expected to have a higher thermal enhancement than the one with hexagonal BN, due to the difference in their thermal conductivity. Also, at very low particle volume concentrations (0.025%) the enhancement in thermal conductivity was found to be much higher than the ones with higher particle volume concentrations. This abnormal increment in thermal enhancement was explained by heat transferred along the aggregated nanoparticles within the nanofluid (percolation mechanism). According to the study of Zhi *et al.* (2011), nanofluids containing boron nitride nanotubes (BNNTs) and boron nitride nanospheres (BNNSs) dispersed in water are found to be highly conductive. Nanofluids are stabilized by using polydiallyldimethylammonium chloride (PDDA) as a surfactant. In this study nanofluids containing both BNNTs and BNNSs are proposed as a remarkable alternative to more common ones containing Al_2O_3, SiC, or CuO due to their high thermal conductivity enhancement and their relatively lower viscosity.

A rheological study of hBN-polyalpha olein oil nanofluids was carried out by Sleiti (2011). In this study, nanofluids with 70 nm sized hBN particles with particle volume concentration from 0.6% up to 1% was tested in the shear rate range of 100-12000 s^{-1} and all tested nanofluids are found to exhibit Newtonian behavior at various temperature values (-20^{o}C to 10^{o}C). Another study by Taha-Tijerina *et al.* (2012) reported Newtonian behavior for hBN-MO nanofluids using two dimensional nano-flakes instead of nanoparticles. Other studies investigating hBN nanofluids do not include any study in regards to rheological behavior. Furthermore, in the study of Zhi *et al.* (2011), nanofluids are prepared by BNNTs and BNNSs and water. They found that the viscosity and thermal conductivity of nanofluids containing BNNTs is higher than the one with BNNSs. Since the increase in the viscosity is an undesired effect of nanoparticle addition to the fluid, nanofluids containing both BNNTs and BNNSs are prepared in order to solve the viscosity problem.

1.3. Convective Heat Transfer Behavior of Nanofluids

As nanofluids are proposed as next generation heat transfer fluids, their convective heat transfer behaviors are also important. Since their possible applications involve their convective heat transfer properties, there have been numerous studies about the convective heat transfer behavior of nanofluids.

In the study of Wen and Ding (2004), Al_2O_3 nanoparticles with a size range of 27-56 nm are suspended into DI water and Nusselt number along the entrance region of a tube under laminar flow conditions, for different Reynolds numbers is presented. It is asserted that in the entrance region, heat transfer enhancement is remarkably higher than the one for base fluid and it decreases along the tube. For 1.6% particle volume concentratio of Al_2O_3-water nanofluids ~41% and ~47% thermal enhancement is obtained at Reynolds number of 1050 and 1600 respectively. Ding *et al.* (2006) conducted an experiment for CNT suspended nanofluids and a remarkable thermal enhancement is observed for 0.5% weight

concentration that is 3.5 times greater compared to the base fluid. However, in the study of Jung *et al.* (2009), convective heat transfer experiments within microchannels were conducted and Al_2O_3 nanoparticles suspended both in DI water and DI water-ethylene glycol mixture show no abnormal heat transfer enhancement for 1.8% volume concentration. These contradictions and abnormal behaviors are reported annually, since nanofluids subject is a popular topic of debate.

1.4. Objective

Considering the literature, there is no prior study that presented preparation of water based nanofluids with hBN nanoparticles. Moreover, there is no study presenting the rheological behavior and thermal conductivity of water based nanofluids with hBN nanoparticles. Therefore, the objective of this study is to prepare stable dispersions by using hBN nanoparticles, and DI water and EG as a base fluid. In order to acquire stability, treatments such as ultrasonication, pH control and surfactant additives are used. The stability level of prepared dispersions is determined by measuring zeta potential and sequential imaging. The existence of agglomerates within the samples is observed by measuring particle size using DLS technique. Also, ESEM and STEM images are used to control agglomeration level within nanofluids. Prior to preparation of hBN nanofluids, two-step preparation method together with use of characterization techniques are validated by preparing and characterizing Al_2O_3 nanofluids that is well documented in the literature. Once stable hBN nanofluids are prepared, their rheological behavior and thermal properties are investigated experimentally. Furthermore, a convective heat transfer setup is constructed to measure heat transfer coefficient of nanofluids. The setup is calibrated with experiments using water and the validity of its results is tested by comparing the results with the one obtained from Shah correlation.

2. METHODOLOGY

2.1. Experimental Procedure

2.1.1. Nanofluid Preparation

70 nm sized hBN nanoparticles with 99.5% purity and 15 nm sized γ-Al_2O_3 nanoparticles that have been purchased from MK Impex Corp., Canada are used in the sample preparation procedure. γ-Al_2O_3 water nanofluids are prepared to validate preparation process and hBN nanoparticles are mixed with both DI-water and EG. In the preparation procedure, desired amount of nanoparticles are first weighed on precision balance (Kern PFB) with ±10 mg accuracy. pH adjustment is a widely adopted method to achieve electro kinetic stability of the suspensions. In the pH study, the base fluid's pH is adjusted by adding hydrochloric acid (HCl) for decreasing the pH, or potassium hydroxide (KOH) for increasing the pH. The pH is then measured using a pH meter (Hanna HI-98107) with ±0.1 accuracy. After adjusting the desired pH of the base fluid, nanoparticles are slowly added to the base fluid while the suspension is mixed by using mechanical homogenizer. The suspension is stirred for 30 minutes with 2015 rpm with the mechanical homogenizer in order to ensure that all the nanoparticles within the base fluid are wetted. Following this procedure, stirred suspension is immediately taken to the sonicator (Hielscher UP400S) for 1 to 6 hours depending on the nanofluid type. The sonication process is performed within a temperature controlled bath to prevent boiling of the base fluid. Hexagonal BN nanofluids with 0.5 to 3% volume concentration are prepared by using either DI-water or EG or both.

In the preparation of hBN nanofluids with surfactant addition, the same weighing procedure for nanoparticles and base fluid is applied. Also, the desired amount of

surfactant is weighed on the precision balance. After this procedure, the surfactant is added to the base fluid while it is mixed by with mechanical homogenizer at 2015 rpm, for 10-15 minutes. During this mixing procedure, formation of foam layers observed and surfactant cannot be dissolved within the base fluid. Samples are kept at the room temperature until the foam at the surface of the sample deflates, then sonication procedure is started. In order to obtain a transparent solution, the surfactant-base fluid suspension is then sonicated 60% amplitude for 15-30 minutes until the surfactant is dissolved. After obtaining a surfactant-base fluid solution, the same procedure for nanoparticle addition and sonication is employed as in the pH study. hBN nanofluids with GA and SDS addition at volume concentrations of 1, 2, and 3% are prepared and they are characterized as explained in the next section.

2.1.2. Characterization

In order to determine the agglomeration and stability of nanofluids both particle size and zeta potential measurements are taken by using particle size and zeta potential analyzer, Brookhaven 90 Plus. For these measurements, nanofluids are diluted to ~0.001% volume concentration and then ~2 ml samples are poured into rectangular prisms shaped polystyrene vessels. All measurements are taken at 25^{o}C.

Furthermore, in order to inspect agglomeration of nanoparticles within the nanofluids visually, methods such as ESEM and STEM imaging are used. ESEM measurements are taken only for dry nanoparticles to determine the nanoparticle agglomerations and compare the particle size with the one that is reported by manufacturer, before it is introduced to the base fluid. STEM imaging is used for characterization of shape and size of nanoparticles within the nanofluids. This method has a drawback compared to the particle size measurement by using DLS method. Nanoparticles cannot be monitored within the liquids, and it is possible to observe them, only after drying. However, shapes of

nanoparticles can be visualized by STEM images which are reported to be very crucial in the determination of rheological behavior of nanofluids (Ding *et al.*, 2010).

Thermal conductivity of hBN and Al_2O_3 nanofluids is assessed by transient hot wire method using a Decagon KD2Pro thermal conductivity analyzer. The thermal conductivity analyzer employed for this study uses a needle which is inserted into the suspension. A heat pulse is applied to the needle and the temperature change is monitored from the needle probe. The behavior of temperature change is dependent on the nature of the medium where the needle probe is inserted. During the measurements, it is intended to measure temperature change assuming that heat transfer is only due to conduction. In the thermal conductivity measurements of fluids with low viscosity, buoyancy driven currents within the fluid can be observed if the needle's temperature is different than the fluid's temperature. This can lead to natural convection driven heat transport introducing error to the measurements.

In order to provide stable environmental conditions, all windows and doors are closed and the prepared nanofluid samples are placed in a water bath. The temperature of the water bath is controlled by using a circulating chiller. Orientation of the probe is crucial in order to take accurate measurements. Probe of the device should be fully placed into the test sample in vertical orientation. The test setup for the thermal conductivity can be seen in Figure 2.1.

In order to investigate the rheological behavior of nanofluids, a cone-plate rheometer (Brookfield DV-III Ultra) is used. Standard plates with 1^o and 3^o cone angle are employed to measure viscosity and shear stress, with respect to shear strain rate that the nanofluids are exposed to. Plate with 1^o cone angle is used for water based nanofluids, whereas the viscosity of EG based nanofluids is investigated by using the 3^o cone plate. Temperature is controlled during all rheological measurements. The accuracy of the measurement changes

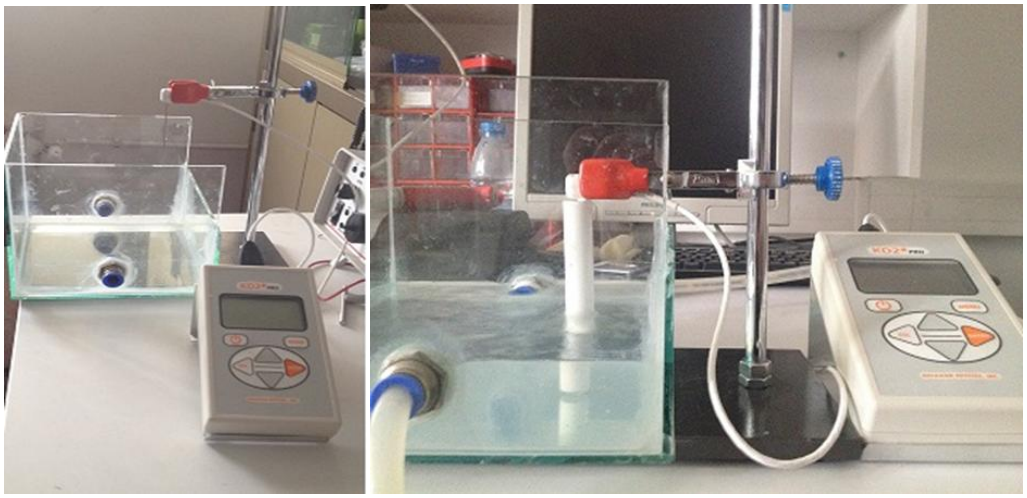

Figure 2.1. KD2 Pro thermal conductivity analyzer and the test setup.

with the shear rate and the viscosity range of the cone plate for the shear rate. Since the torque measurement accuracy is 1% of full scale range, for example, if the viscosity range is up to 10 mPa·s for the applied shear rate and the cone plate used during the experiment, the uncertainty of the measurement is ±0.1 mPa·s. For spindle with 1^{o} cone angle, at 75 s^{-1} shear rate, the viscosity range is specified as up to 300 mPa.s, so the accuracy of measurement at this shear rate is ±3 mPa.s.

2.2. Transient Hot Wire Method

In transient hot wire method, a very thin, infinitely long line source dissipates heat in an infinite and incompressible medium and the temperature increase in the medium can be observed along time assuming that the heat source has an infinite thermal conductivity and zero heat capacity, and all generated heat is transferred to the medium by conduction alone (Simham, 2008). One dimensional heat conduction equation in cylindrical coordinates:

$$\frac{1}{\alpha_f}\frac{\partial T}{\partial t}=\frac{1}{r}\frac{\partial}{\partial r}\left(r\frac{\partial T}{\partial r}\right) \tag{2.1}$$

where considering that $T=T_o+\Delta T$ in Equation 2.1 where the temperature of the medium is a function of time t and the radial coordinate r, and α_f is the thermal diffusivity of the fluid. Considering that $T=T_o+\Delta T$ where T_o is the initial temperature of the medium, and ΔT is the transient temperature change in the medium. If the boundary conditions are applied to Equation 2.1 (Simham, 2008):

$$\lim_{r\to 0}\left\{r\left(\frac{\partial T}{\partial r}\right)\right\}=-\frac{q'}{2\pi k_f} \quad \text{at } t=0 \text{ and } r=0 \tag{2.2}$$

$$\lim_{r\to\infty}\{\Delta T(r,t)\}=0 \qquad \text{at } t\geq 0 \text{ and } r=\infty \tag{2.3}$$

where k_f is the thermal conductivity of the liquid medium and q' is the heat per length of the wire. As it is stated in Equation 2.2, temperature gradient at $r=0$ is constant, in other words the system is at thermal equilibrium before heater is turned on. Furthermore, temperature difference at the infinity is equal to zero while the system is heating up as it is given in Equation 2.3. The solution of this problem is presented in Carslaw and Jaeger (1959) as:

$$\Delta T(r,t)=T(r,t)-T_o=\frac{q}{4\pi k_f}\mathrm{Ei}\left(\frac{r^2}{4\alpha_f t}\right) \tag{2.4}$$

Equation 2.4 represents the temperature change within medium from initial temperature T_o at an arbitrary distance r, after a particular time t. The left part of Equation 2.4, represents temperature change in time due to heating. The series expansion of the exponential integration at the left hand side is given as,

$$\mathrm{Ei}(\gamma) = -\gamma - \ln(\gamma) - \sum_{z=1}^{\infty} \frac{(-1)^z (\gamma)^z}{z \cdot z!} = -\gamma - \ln(\gamma) + \left[\frac{\gamma}{1 \cdot 1!} - \frac{\gamma^2}{2 \cdot 2!} + \frac{\gamma^3}{3 \cdot 3!} - ..... + ... \right] \quad (2.5)$$

where $\gamma = 0.5772$ is the Euler's constant.

After several mathematical steps, for very large intervals of time, Equation 2.5 can be derived into,

$$\Delta T(r,t) = T(r,t) - T_o = \frac{q}{4\pi k_f} \left\{ -\gamma + \ln\left(\frac{4\alpha_f t}{r^2} \right) \right\} \quad (2.6)$$

Thus, at an arbitrary radial distance r, temperature difference at two different time can be written as,

$$\Delta T_2 - \Delta T_1 = \frac{q}{4\pi k_f} \ln\left(\frac{t_2}{t_1} \right) \quad (2.7)$$

Equation 2.7 shows that the temperature difference in a specific time interval is independent from radial effects. Therefore, if the temperature change in the medium and

logarithmic time scale is plotted, the slope of the obtained line can be described as thermal conductivity of the medium:

$$k_f = \frac{q}{4\pi} \frac{d\ln(t)}{d\Delta T} \tag{2.8}$$

The advantage of this method is the elimination of the effect of radial distance, thus the linear dependency between temperature increase and the logarithmic time change can be accomplished.

2.3. Viscosity Measurements

In this study, Brookfield DV-III Ultra cone/plate rheometer, which is a rotational viscometer, is used. The rheological data is analyzed by using Brookfield RheocalcSoftware32.

Cone-plate is probably the most used geometry in rheological investigation. A schematic of cone plate geometry is given in Figure 2.2. Assuming the flow between conic spindle and the plate is steady, laminar, and isothermal with negligible gravity and end effects; one can describe equations of motion in spherical coordinates (r', θ, ϕ) as in Equation 2.9, 2.10 and 2.11, respectively. While writing these equations, it is used that the velocity in the radial and vertical directions are zero ($v_{r'} = v_z = 0$), and cone angle, θ_0, is lower than 0.1 rad ($\theta_0 \leq 0.1 \text{rad.}$). The flow is only in ϕ direction dependent on the directions of r and θ, $v = v_\phi(r', \theta)$.

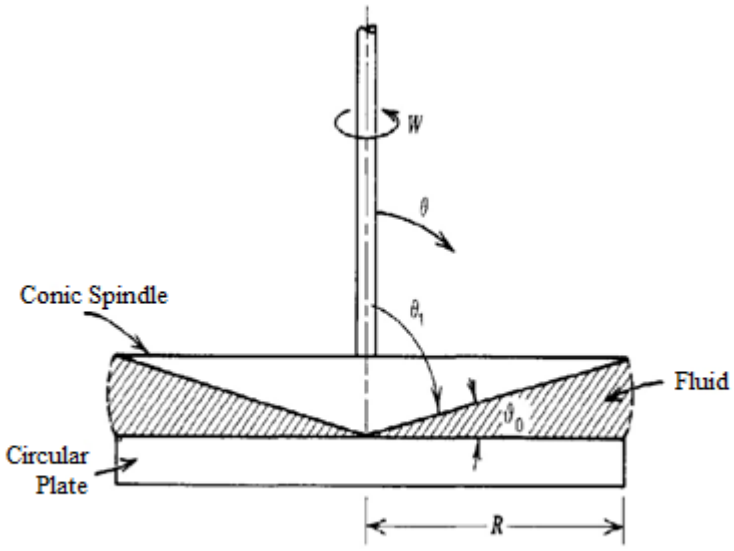

Figure 2.2. Cone and plate rheometer (Bird, 1987).

$$\frac{1}{r^2}\frac{\partial(r^2\sigma_{rr})}{\partial r}-\frac{\sigma_{\theta\theta}-\sigma_{\phi\phi}}{r}=-\rho\frac{v_\theta^{\,2}}{r} \tag{2.9}$$

$$\frac{1}{r\sin\theta}\frac{\partial(\sigma_{r\theta}\sin\theta)}{\partial r}-\frac{\cot\theta}{r}\cdot\sigma_{\theta\theta}=0 \tag{2.10}$$

$$\frac{1}{r}\frac{\partial\sigma_{\theta\phi}}{\partial\theta}+\frac{2}{r}\cot\theta\cdot\sigma_{\theta\phi}=0 \tag{2.11}$$

In Equation 2.9, 2.10, and 2.11; r, θ, and ϕ are the spherical coordinates; $\sigma_{\theta\phi}$ represents stress tensor in θ and ϕ coordinates; and v_θ is the velocity of fluid in θ direction. Since the velocity at the tip of the spindle is equal to zero, and the velocity along the conic surface of the spindle is approximately equal to the velocity at the spindle,

$$v_{\phi}\left(\pi/2\right)=0 \tag{2.12}$$

$$v_{\phi}\left(\pi/2-\theta_0\right)=\omega r\sin\left(\pi/2-\theta_0\right)\approx\omega r \tag{2.13}$$

boundary conditions can be written as in Eqns 2.12 and 2.13. ω is the rotational velocity of the spindle. One can re-write Equation 2.11 by considering these boundary conditions as,

$$\sigma_{\theta\phi}=\frac{C}{\sin^2\theta}\cong cst \tag{2.14}$$

The shear stress is a constant value dependent only on θ, since the conic angle is a sufficiently small value. One can write the applied torque to the rheometer as;

$$M=\int_0^{2\pi}\int_0^{R} r^2\sigma_{\theta\phi}\,dr\,d\phi \tag{2.15}$$

In Equation 2.15, M is the applied torque to the spindle. By combining Equation 2.14 and 2.15, shear stress can be written as,

$$\sigma_{\theta\phi}=\frac{3M}{2\pi r^3} \tag{2.16}$$

From the Equation 2.16, it can be asserted that shear stress at $\theta - \phi$ is independent of the flow characteristics, dependent only on r and M. Furthermore, it can be asserted that the shear rate is homogeneous and constant throughout the sample as it is given in Equation 2.17.

$$\dot{\gamma} = \frac{\mathrm{v_r}}{\mathrm{h(r)}} = \frac{\omega \cdot \mathrm{r}}{\mathrm{r} \cdot \mathrm{tg}(\theta_0)} = \frac{\omega}{\mathrm{tg}(\theta_0)} \cong \frac{\omega}{\theta_0} \tag{2.17}$$

In Equation 2.15, $\dot{\gamma}$ is shear stress, h(r) is the vertical distance between conic spindle surface and plate. Since $\theta_0 \leq 0.1\mathrm{rad}$, shear stress can be written in a simple form, dependent only on rotational velocity and conic angle as in Equation 2.15. Thus, in cone plate rheometers, rotational velocity, conic angle and applied torque are known values, shear stress and shear rate can easily be measured according to the theory presented below.

Rheometers operate as a sensitive torquemeter that collects data in a specific range of rotational velocity (0.01-250 rpm). The sample is placed between the spindle, the moving part at the very end of the rheometer, conic part and the plate. The resistivity of the sample against the rotation of the spindle is sensed by a very sensitive spring system and as a result torque measurement is accomplished.

The resistance measured by conic spindle and the frictional stress on the surface of the sample are proportional. Therefore, the viscosity data can be obtained according to this proportion by using software of the rheometer. Furthermore, the viscosity of the fluid can be obtained analytically by using geometric dimensions of the conic spindle, and the values of the torque and rotational velocity measured by the rheometer.

The stable plate in which the sample is planted can be disassembled and reassembled. The amount of the sample varies depending on the conic spindle used for the viscosity measurement (0.5-2 ml). There is no need for the calibration during the replacement of rheometer plate. In the viscosity measurement, the spindle models CPE 40 is used for low viscosity measurements and CPE 41 for higher ones.

The gap between the spindle and the rheometer is the most important parameter during the measurement. The conic spindle should be fully interacted with the surface of the fluid, not be located underneath the surface. This gap can be calibrated by the "auto-zero" function of the rheometer.

2.4. Convective Heat Transfer Setup

2.4.1. Experimental Setup

The purpose of the convective heat transfer setup is to experimentally investigate the enhancement of heat transfer due to internal forced convection of a nanofluid subject to constant heat flux at boundaries.

The schematic of convection test setup is presented in Figure 2.4. Basically, fluid runs in a loop where it is first heated and then cooled continuously. Before it enters the test section, the fluid first passes through the flowmeter, which is used to measure the volumetric flow rate of the fluid. A turbine flowmeter is used that has a digital output signal which is processed using an Arduino card. In the inlet and outlet of the test section; two pressure transducers are placed to measure the pressure drop along the test section which output an analog signal, between 0.1 V and 5.1 V. They need a power input to operate and they can be supplied with a voltage between 12V and 28V. Input signal does not affect the

output signal, but calibration of these equipments is employed at 20 V. The inlet pressure transducer (Setra 206) has a measurement range of 0-50 psig; whereas the exit pressure transducer (Setra 206) has a measurement range of 0-25 psig. The accuracy of pressure transducers are ±0.13% of the measured value. The accuracy of the flowmeter is ±1% of the measured value.

The heat section is constructed with 1.5 m long aluminum tube with 4 mm inner and 6 mm outer diameter and it comprised of two parts. The first 0.5 m the fluid flows with no heat-up so that the flow develops. Heating unit is comprised of a bare nichrome wire resistance, firmly wrapped around the taped pipe to obtain uniform heat flux around the pipe. Electric isolation tapes are used in between the pipe and heater wire to prevent any current leaking from heater wire to the fluid. Furthermore, in order to minimize the heat loss, heating unit is

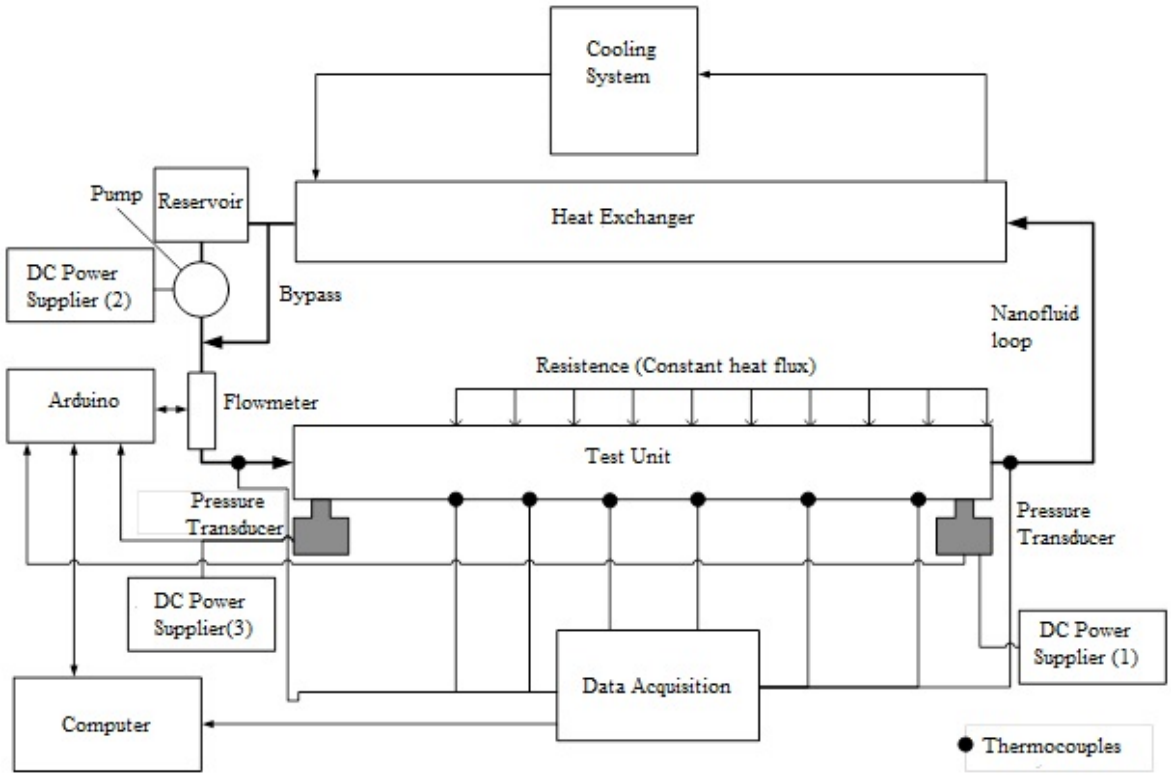

Figure 2.3. Schematic of convection test setup.

Figure 2.4. Pressure transducer connected to the test setup.

isolated. In this experimental setup, heat transfer coefficient of a fluid can be identified by variation of mean temperatures variation along heating section, and surface temperature distribution along the pipe. T-type thermocouples with special measurement accuracy ($\pm 0.5^{o}C$) are used to measure surface temperatures along the pipe. Mean temperatures are measured at the inlet of the pipe and local mean temperatures are estimated based on inlet temperatures and applied heat flux. Data acquisition system, Agilent 34970A, is employed to monitor temperature data.

There are seventeen T-type thermocouples used within the test setup. Fifteen of them are used on the surface of the pipe and two of them are used to measure inlet and outlet temperature of the heating section. In this study, thermocouple attachment poses a great challenge because, the heater resistance wire is too close to the attached thermocouples and during the experiments, thermocouple detachment from the surface occurs due to excessive local heat-up. Furthermore, as the thermocouples and the heater are too close to each other, abnormally high temperature measurements might be taken. After several experiments with Kapton tape, epoxy, and Cerastil in order to ensure firm attachment to the surface of the pipe, the best temperature results are achieved with super glue. Attachment materials other than super glue are not effective because it takes several hours for them to dry and in this time period, thermocouple beads start to detach from the surface.

After the heating unit fluid arrives at the cooling unit that is used to sustain steady state operation of the system. The cooling unit is comprised of a counter flow concentric tube heat exchanger. The heated fluid passing through the inner tube is cooled by cold water flowing outside. A reservoir and a centrifugal pump are placed where the loop finishes. There are two valves used in the test setup; one of them is just after the pump in order to control the flow rate, the other one is located at the bypass line which can be used to arrange flow rate as well.

Except for the heating and cooling unit, the remaining part of the loop is constructed with silicone pipes because of their easy implementation and transparency. Bubbles in the loop can be observed from outside, to ensure degassing. Silicone is selected because of its high temperature resistance up to 300^{o}C. In order to connect silicone pipes to heating and cooling section and attached equipments, brass connectors are used. Brass is chosen because of its resistivity to corrosion.

Table 2.1. Position of T-type thermocouples.

Thermocouples	x[m]
1	0
2	0.05
3	0.1
4	0.15
5	0.25
6	0.35
7	0.43
8	0.5
9	0.65
10	0.75
11	0.8
12	0.85
13	0.9
14	0.95
15	1

There are two valves in the setup, one is located just after the pump to control flow rate, the other one is at the by-pass line to degas the fluid and control flow rate as well. Reservoir is placed just before the pump in order to charge the system, and avoid the pump from running dry. Furthermore, it is effective for degassing the flow as well.

The system must be charged with the reservoir, as running dry will damage the pump. In order to utilize gravity for charging, the pump is clamped 20 cm lower than the reservoir. When it is turned on, in order to eliminate the bubbles within the test setup, bypass line is opened. When the degassing of the system is achieved, the sound of pump noise reduces.

Figure 2.5. The pump and the reservoir.

2.4.2. Theory

The convective heat transfer coefficient of the fluid is calculated through the temperature measurements on the heated aluminum pipe. The local heat transfer coefficient is calculated along the pipe throughout the thermal entry region until it converges to the fully developed value.

Nusselt number is a non-dimensional value that compares the convective heat transfer capability to the conductive heat transfer capability. Local Nusselt number is defined as:

$$Nu_x = \frac{h_x D}{k_f} \tag{2.18}$$

where h_x is local heat transfer coefficient, k is the thermal conductivity, and D is the inner diameter of the pipe. For fully developed laminar flows subjected to a constant surface heat flux, the Nusselt number is theoretically 4.36. Local heat transfer coefficient along a pipe heated with constant heat flux can be defined as,

$$h_x = \frac{q''}{T_{s,x} - T_{m,x}} \tag{2.19}$$

In Equation 2.19, q'' is the surface heat flux, $T_{s,x}$ is the local surface temperature along the pipe, and $T_{m,x}$ is the local mean temperature along the pipe. By introducing, $T_{m,x}$ as,

$$T_{m,x} = T_{m,i} + \frac{q'' Px}{\dot{m} c_p} \tag{2.20}$$

to the Equation 2.19, h_x can be re-written as,

$$h_x = \frac{q''}{T_{s,x} - T_{m,i} - \frac{q'' Px}{\dot{m} c_p}} \tag{2.21}$$

where $T_{m,i}$ is the inlet mean temperature, P is the perimeter of the pipe, x is the position along the pipe, $\dot{m}$ is mass flow rate of the fluid, and c_p is the heat capacity of the fluid. According to Equation 2.21, one can calculate local heat transfer coefficients along a pipe heated with a constant heat flux, if the mass flow rate, inlet mean temperature and surface temperature distribution along the pipe are known. In the convection heat transfer setup, the local heat transfer coefficient of a fluid will be estimated based on these measured quantities. Furthermore, the Nusselt number as a function of axial distance is calculated from the measured temperature and flow rate values.

$$Nu_x = \frac{q''}{T_{s,x} - T_{m,i} - \frac{q'' \pi D x}{\dot{m} c_p}} \frac{D}{k_f} \tag{2.22}$$

as the perimeter of the pipe, $P = \pi D$.

The measured values of surface temperature are compared with the values calculated from Shah correlation in order to calibrate test setup with DI water. Shah correlation for laminar flows is given as in Equation 2.23.

$$\begin{aligned} Nu_x &= 1.953 \left(Re\, Pr \frac{D}{l} \right)^{1/3} \quad \text{for} \quad \left(Re\, Pr \frac{D}{l} \right) \geq 33.3 \\ Nu_x &= 4.364 + 0.0722\, Re\, Pr \frac{D}{l} \quad \text{for} \quad \left(Re\, Pr \frac{D}{l} \right) \prec 33.3 \end{aligned} \tag{2.23}$$

where Nu_x is the local Nusselt number, Re is the Reynolds number, Pr is the Prandtl number, and l is the length of the pipe.

2.4.3. Uncertainty Analysis

Single sample uncertainty analysis is used in order to understand the validity of the collected data from convection test setup. The measurement uncertainty of Nu_x is,

$$S_{Nu_x}{}^2 = \left(\frac{\partial Nu_x}{\partial \dot{m}} S_{\dot{m}}\right)^2 + \left(\frac{\partial Nu_x}{\partial T_{s,x}} S_T\right)^2 + \left(\frac{\partial Nu_x}{\partial T_{m,i}} S_T\right)^2 + \left(\frac{\partial Nu_x}{\partial q''} S_{q''}\right)^2 \quad (2.24)$$

where S_i represents uncertainty for the measurement of i. Although, the heat unit is insulated; the system is still prone to heat loss. The heat flux applied to the system can be defined as,

$$q'' = \frac{\dot{m} c_p}{Pl}(T_{m,o} - T_{m,i}) \quad (2.25)$$

and the uncertainty for the heat flux can be defined as,

$$S_{q''}{}^2 = \left(\frac{\partial q''}{\partial \dot{m}} S_{\dot{m}}\right)^2 + \left(\frac{\partial q''}{\partial T_{m,i}} S_T\right)^2 + \left(\frac{\partial q''}{\partial T_{m,o}} S_T\right)^2 \quad (2.26)$$

where $T_{m,o}$ is the outlet mean temperature. Also, since the measured value is volume flow rate other than mass flow rate, the uncertainty of mass flow rate can be calculated accordingly,

$$S_{\dot{m}}{}^2 = \left(V_f \cdot S_\rho\right)^2 + \left(\rho \cdot S_{V_f}\right)^2 \tag{2.27}$$

$$\dot{m} = \rho V_f \tag{2.28}$$

Equation 2.27 is the definition of uncertainty of mass flow rate and Equation 2.28 is the definition of mass flow rate. In these equations V_f is the volume flow rate and ρ is the density of the fluid. By inserting Equation 2.26 and 2.27 into 2.24, and knowing that the measurement uncertainty for T-type thermocouples is 0.5 K, $S_T = 0.5\text{K}$, and for volumetric flow rate, 1% of the measured value, $S_{V_f} = V_f/100$, the measurement uncertainty of local heat transfer coefficient can be calculated.

3. RESULTS AND DISCUSSION

The objective of this study is to identify required parameters to prepare stable hBN nanofluids and characterize their thermal and rheological properties. Besides, a construction of convective heat transfer setup to investigate local heat transfer coefficient of nanofluids is another purpose of this study. Therefore, Al_2O_3 and hBN nanofluids are prepared by changing parameters such as sonication time, pH level, surfactant type and volume concentration, and particle volume concentration to achieve stable dispersions. The effects of these parameters on stability evaluated in terms of zeta potential, particle size of nanoparticles, and qualitative imaging for the nanofluids are presented.

A validation study for Al_2O_3-water nanofluids of 0.5, 0.75, and 1% volume concentration is executed first. Following the validation study, hBN-water/EG nanofluids are investigated. ESEM images for hBN and Al_2O_3 nanoparticles are taken to determine the agglomeration level before mixing. In addition, images of hBN-EG with 0.5% volume concentration and Al_2O_3-water nanofluids are taken to investigate agglomeration of nanofluids qualitatively. Examination of rheological behavior of hBN-water, hBN-EG, hBN-water-EG and Al_2O_3-water nanofluids is performed under controlled thermal conditions by changing shear rate in a suitable range for each of the nanofluid. Following this procedure, thermal conductivity of these nanofluids is investigated and thermal conductivity enhancements of these nanofluids are determined accordingly.

Construction of a convective heat transfer setup is employed to investigate local heat transfer coefficient of nanofluids. The setup is calibrated with DI water and an uncertainty analysis is executed to determine measurement error.

3.1. ESEM and STEM Images

Particle sizes of hBN and Al_2O_3 particles are reported as 70 and 15 nm by the manufacturer. As it can be seen from Figure 3.1 and 3.2 both Al_2O_3 and hBN nanoparticles are agglomerated prior to mixing because of transportation and storage conditions. Especially, hBN nanoparticles are severely agglomerated; almost 500 nm sized particles can be observed in Figure 3.2. Sonication is applied after mixing with base fluid as it is an effective solution to resolve this problem.

Hexagonal BN-EG and Al_2O_3-water nanofluids are prepared by sonicating both suspensions for 3 hours. By using STEM method, images of nanoparticles within nanofluids can be visually investigated. In this method, droplets from examined fluids are introduced to test grids and they are left to dry completely. Images taken for Al_2O_3-water and hBN-EG nanofluids with 0.5% particle volume concentration are presented in Figure 3.3a-c. As it can be seen from Figure 3a, up to 246 nm sized aggregates within for Al_2O_3-

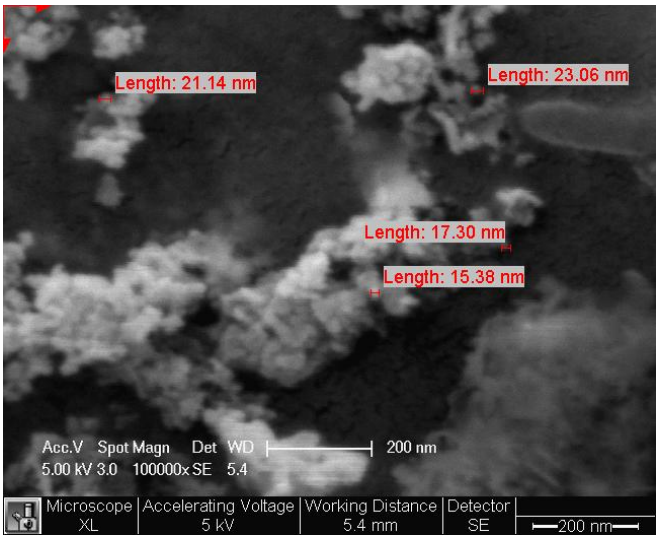

Figure 3.1. ESEM images of dry γ-Al2O3 nanoparticles.

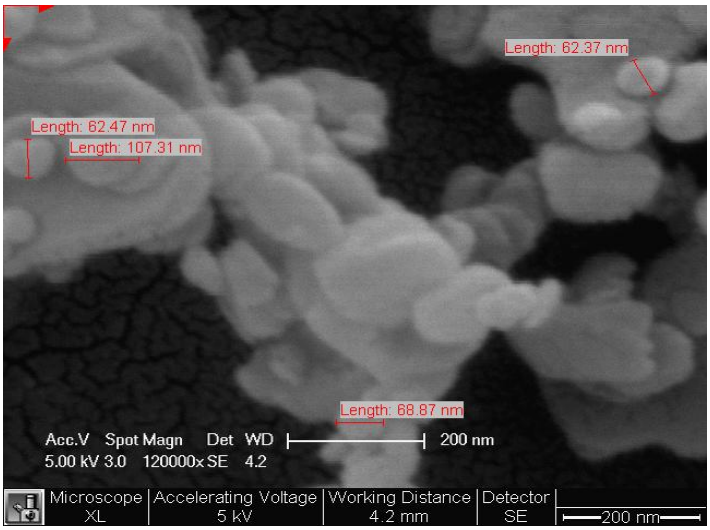

Figure 3.2. ESEM images of dry hBN nanoparticles.

water nanofluids with 0.5% particle volume concentration can be observed. However, for hBN-EG, STEM imaging could not be performed. In the process of grid drying, EG crystallizes and dries, as a result hBN nanoparticles stick to these crystals. As a solution to this problem, dried grids can be visualized by using ESEM. EG crystals can be observed in Figure 3.3b. Figure 3.3c shows that the agglomerations of dry hBN nanoparticles observed in Figure 3.2 are eliminated in EG.

3.2. Al_2O_3- Water Nanofluids

3.2.1. Preparation and Stability of Al_2O_3- Water Nanofluids

Before starting preparation of hBN nanofluids, a comparison with 1 hour sonicated Al_2O_3-water nanofluids at pH 7 and the data taken from the study of Lai (2010) is presented. In

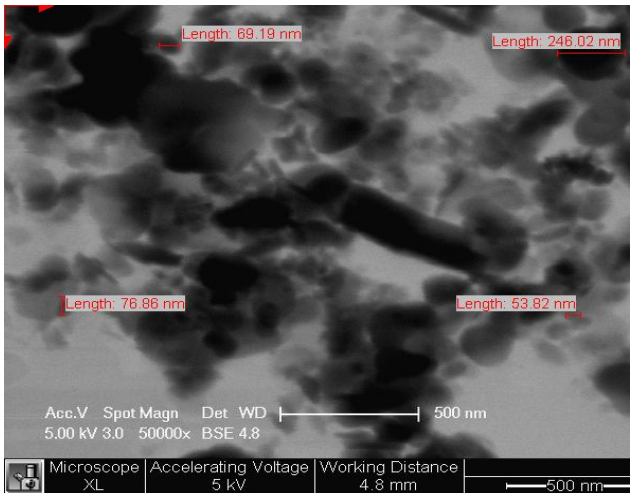

(a)

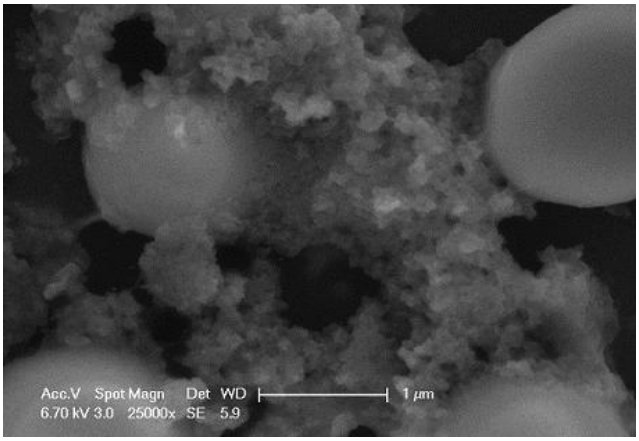

(b)

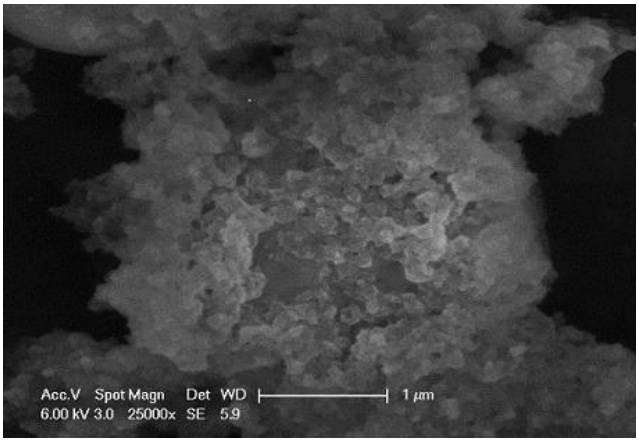

(c)

Figure 3.3. STEM images Al_2O_3-water(a) and hBN-EG nanofluids(b,c) with 0.5% volume concentration.

this study zeta potential of these samples are measured along 60 minutes, as shown in Figure 3.4. This particular preparation method for Al_2O_3-water nanofluid replicates the literature (Lai, 2010). As it is presented in Figure 3.4, measured values for particle volume concentrations of 0.5 and 0.75% are in a good agreement with data from literature (Lai, 2010). Zeta potential measurements for Al_2O_3-water nanofluid with 0.5% particle volume concentration indicates that the suspension is stable with a zeta potential value of approximately 45 mV for 1 hour sonication which means good stability. Whereas, zeta potential of the nanofluid sample with 1% particle volume concentration decreases to approximately 30 mV which indicates incipient stability. Therefore, Al_2O_3-water nanofluid prepared as 1% particle volume concentration need to be sonicated more than 1 hour to prevent agglomeration and sedimentation within the nanofluids.

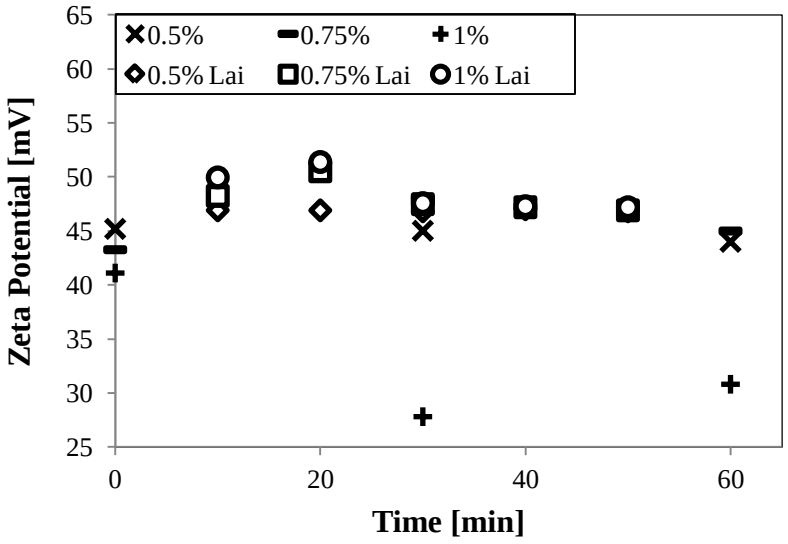

Figure 3.4. Comparison of zeta potential for Al_2O_3-water nanofluids synthesized in this study and literature (Lai, 2010).

3.2.2. Rheological Behavior of Al_2O_3-Water Nanofluids

After characterization of Al_2O_3-water nanofluids, a rheological study to investigate the behavior of them under variable shear rate is performed. For all three volume concentrations, test fluids are sonicated for 3 hours and the pH is adjusted to 4.5. Zeta potential values are varied between 50 to 55 mV which implies that the dispersions remain stable during the measurements. According to Figure 3.5, Al_2O_3-water suspensions display Newtonian behavior as it is reported in several other studies (Buongiorno *et al.*, 2009; Prasher *et al.*, 2006).

Variation of viscosity with respect to the particle volume fraction for Al_2O_3-water nanofluids is shown at Figure 3.6 along with the similar experimental studies (Das *et al.*, 2003, Utomo *et al.*, 2012; Wang *et al.*, 1999) and Einstein's prediction. The viscosity increment is increasing with the increase in the particle loading as it is expected. Einstein's equation is valid for the nanofluids of particle volume concentration less than 2

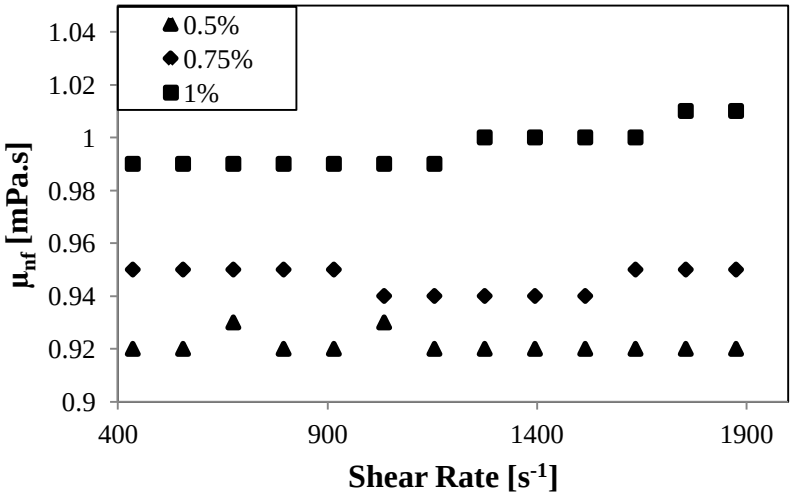

Figure 3.5. Viscosity measurements of Al_2O_3-water nanofluids at variable shear rate for different volume concentrations at the temperature of 24^{o}C.

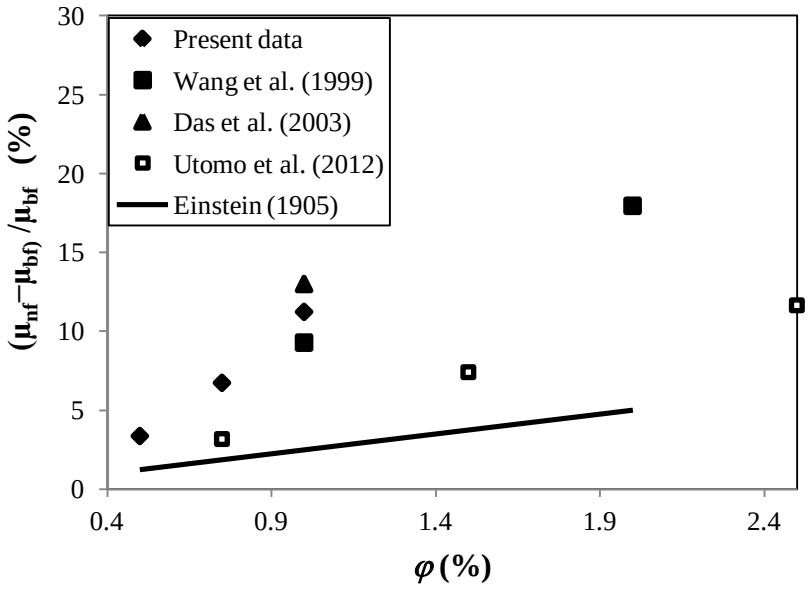

Figure 3.6. Comparison of the viscosity change of the measured data with respect to the base fluid for Al_2O_3-water nanofluids of different volume concentrations with the literature.

% (Einstein, 1905). The increase observed in the present data exceeds the predictions by Einstein's equation (1905) and experimental data taken from Utomo *et al.* (2012), whereas it is similar to the studies of Das *et al.* (2003) and Wang *et al.* (1999).

3.2.3. Thermal Conductivity Measurements for Al_2O_3-Water Nanofluids

Thermal conductivity of the Al_2O_3-water nanofluid samples that are prepared as explained in the previous section are presented in Figure 3.7 in comparison with Al_2O_3-water studies in the literature (Chandrasekar *et al.*, 2010; Li *et al.*, 2007; Mallick *et al.*, 2013; Teng *et al.*, 2010) along with Maxwell model. The measured thermal conductivity enhancements for Al_2O_3-water nanofluids for 1 and 2% volumetric particle concentration

are higher than the ones for other experimental studies. The cause of this result might be adjusted pH of 4.5 of Al_2O_3-water samples during the preparation in order to obtain stability. It should be noted that in other studies (Chandrasekar *et al.*, 2010; Li *et al.*, 2007; Mallick *et al.*, 2013; Teng *et al.*, 2010) pH control is not employed for Al_2O_3-water nanofluids.

3.3. pH Study with hBN-Water Nanofluids

3.3.1. Preparation and Stability of pH Adjusted hBN-Water Nanofluids

After validating the two-step nanofluid preparation method, hBN nanofluids are investigated. As it is indicated before, in zeta potential and effective aggregate size measurements, nanofluids are diluted to 0.001% hBN by volume. The dilution is executed

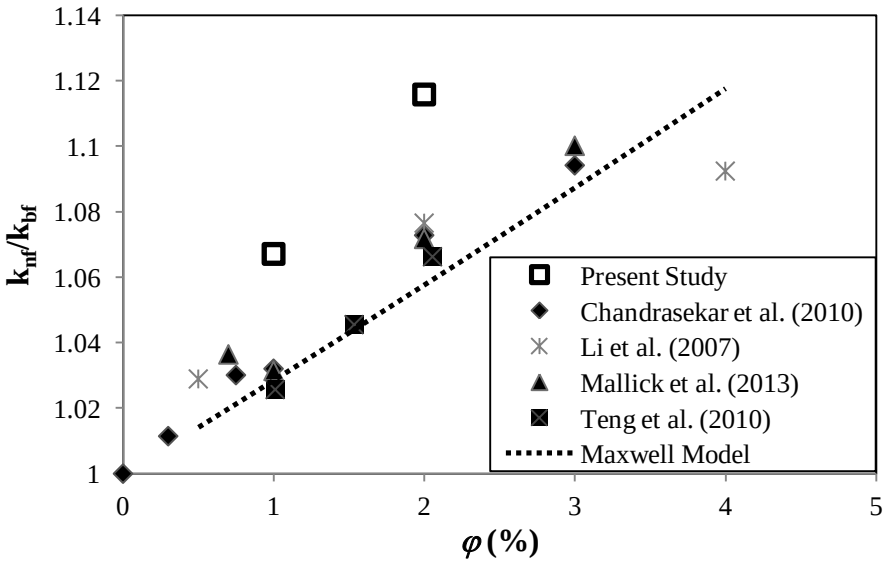

Figure 3.7. Thermal conductivity ratio vs. volume concentration for Al_2O_3-water nanofluids of present study and other studies along with the Maxwell model.

by using DI water at pH 7. Calculated pH of diluted, 5 different 20 ml samples are presented in Table 3.1 along with the measured initial pH of the base fluid of nanofluids with 0.5% hBN by volume before dilution. Zeta potential measurements for hBN-water samples with different pH are shown in Figure 3.8. As it can be seen, by changing the pH electrokinetic repulsive forces can be tuned to provide stable dispersions. According to Figure 3.8, the most stable dispersion is Sample 4 with a zeta potential value of 48.4 mV. Since base fluid of Sample 4 has pH of 12, Sample 1 with a zeta potential value of 43.87 mV is chosen for further investigation in this study. Sedimentation is observed within 30 minutes after sonication for Sample 5, which manifests itself with a zeta potential value of 15 mV.

In the preparation of hBN - water nanofluids, optimal values for both pH and sonication time should be identified. The optimal sonication time can be obtained according to Figure 3.9. Figure 3.9 indicates that the highest zeta potential value is achieved for 3-hour sonication time, whereas the lowest particle size is obtained with 12-hours sonication time. Although the second highest zeta potential value can be reached after 12 hours of sonication, due to the significant time increase, the optimal sonication time for hBN-water nanofluid preparation is considered as 3 hours.

Table 3.1. pH of prepared samples before and after dilution.

Samples	φ [%]	Sonic. Time [hr]	pH (base fluid)	pH (diluted nanofluid)
1	0.5	3	9	7.07
2	0.5	3	10	7.48
3	0.5	3	11	8.32
4	0.5	3	12	9.3
5	0.5	3	13	10.3

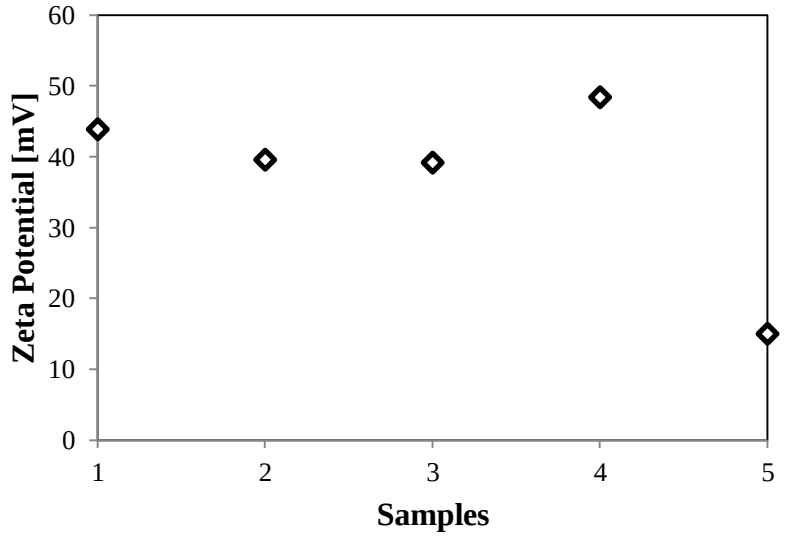

Figure 3.8. Zeta potential measurements for different hBN-water nanofluid samples.

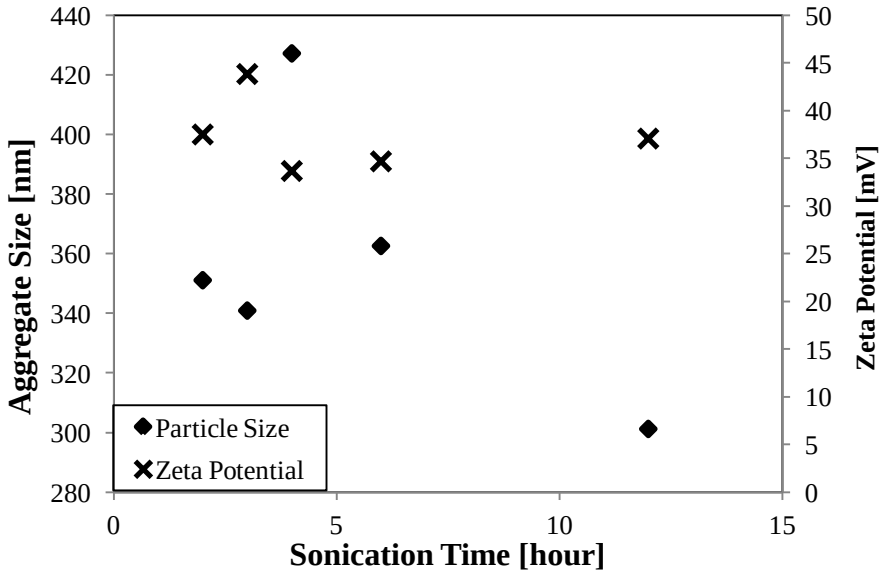

Figure 3.9. Change in zeta potential and particle size of 0.5% hBN-water nanofluids with different sonication time.

Optimized pH and sonication time change with the changing volume concentration. Therefore, similar optimization studies are executed for the other volume concentrations (0.75, 1%). In this study, for 0.5, 0.75, 1% hBN by volume concentrations, optimized sonication time changes with the change in volume concentration whereas the optimized pH for these samples are almost the same, with base fluid pH of either 9 or 12. Preparation procedure for hBN-water nanofluids is summarized for different volume concentrations in Table 3.2.

3.3.2. Viscosity Measurements of pH Adjusted hBN-Water Nanofluids

Volume concentration, sonication time, and base fluid pH, measured zeta potential, aggragate size, and viscosity values are summarized in Table 3.3. According to zeta potential values just after sonication, the pH adjusted hBN-water samples are stable. Aggregate size of these samples are up to ~7 times of the particle size value (70 nm) reported by the manufacturer. Viscosity measurements are performed for the three particle

Table 3.2. Preparation parameters for pH study of hBN-water nanofluids.

φ [%]	Sonication Time [hr]	pH
0.5	3	9
0.75	5	9
1	6	12

Table 3.3. Summary of preparation procedure and measured zeta potential and viscosity data for different volume concentrations of hBN-water nanofluids in pH study.

φ [%]	Sonication Time [hr]	pH (base fluid)	Zeta Potential [mV]	Aggregate Size [nm]	Viscosity [mPa.s]
0.5	3	9	44	340	0.93
0.75	5	9	39	392	0.96
1	6	12	35	435	0.99

volume concentrations and measured values are presented accordingly. During the experiments, the temperature is kept at 24°C. As presented in Figure 3.10, nanofluids with 0.5, 0.75, and 1% hBN by volume exhibit Newtonian behavior in the shear rate range of 187.5-1000 sec^{-1}. Furthermore, viscosity ratio change with particle volume concentration is plotted as in Figure 3.11. Einstein's prediction (1905) clearly underestimates the measured data for all three volume concentrations.

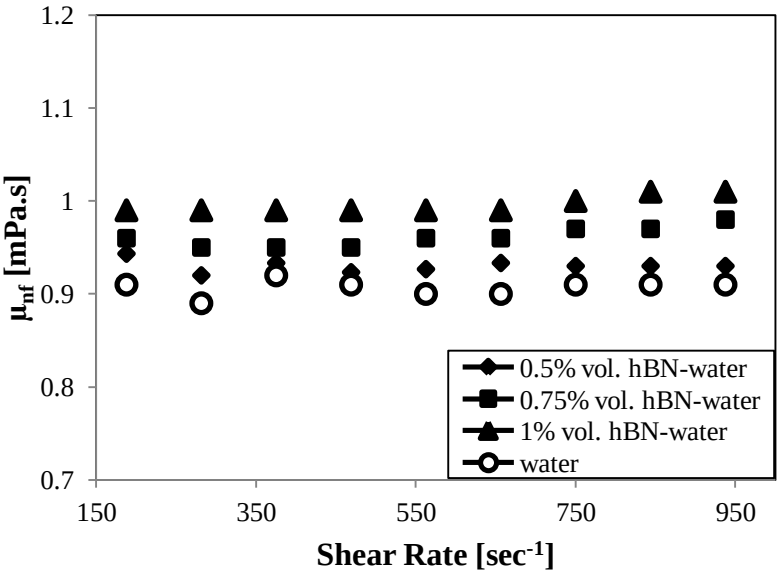

Figure 3.10. Viscosity variation with shear rate of hBN-water nanofluids of various volume concentrations at the temperature of 24°C with the pH values presented in Table 3.3.

3.3.3. Thermal Conductivity Measurements of pH Adjusted hBN-Water Nanofluids

In order to observe the enhancement in thermal conductivity, hBN-water nanofluids with higher volume concentrations (1, 2, 3%) are prepared by adjusting their pH to 12 by using KOH. They are all sonicated for 6 hours. In Table 3.4, their preparation procedure is summarized. After the preparation, their thermal conductivity is measured. As presented

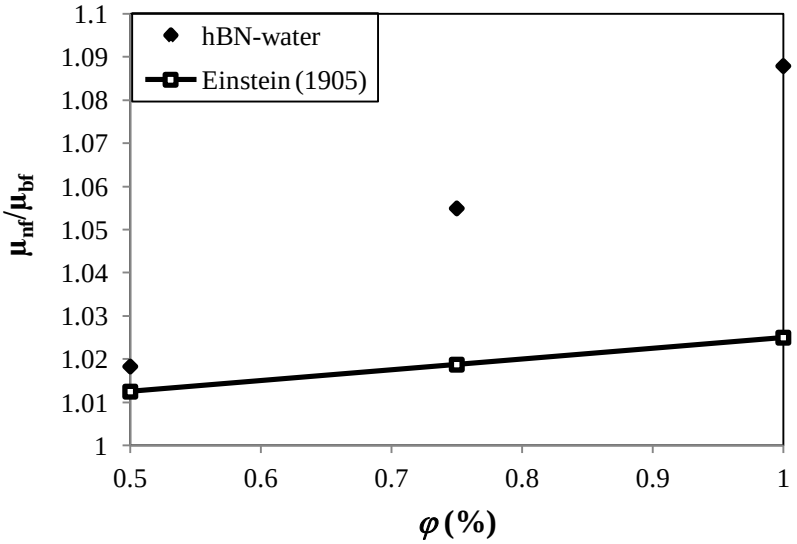

Figure 3.11. Measured viscosity ratio variation of hBN-water nanofluids with volume concentration (at the shear rate of 562.5 s^{-1}).

in Figure 3.12, thermal conductivity of hBN-water nanofluids is higher than the ones measured for Al_2O_3-water nanofluids. Whereas the thermal conductivity ratio (k_{nf}/k_{bf}) for Al_2O_3-water nanofluids with 2% Al_2O_3 by volume is ~10%, hBN-water nanofluids at the same volume concentration has thermal conductivity enhancement ratio of ~20%. Furthermore, for hBN-water nanofluids 3% hBN by volume, 42% thermal conductivity enhancement can be obtained as shown in Figure 3.12. This abnormal enhancement may be the result of both relatively higher thermal conductivity of hBN nanoparticles, and the effect of pH adjustment on hBN-water nanofluids.

Table 3.4. Preparation procedure of hBN-water nanofluids in thermal conductivity measurement section of pH study.

φ [%]	Sonication Time [hr]	pH (base fluid)
1	6	12
2	6	12
3	6	12

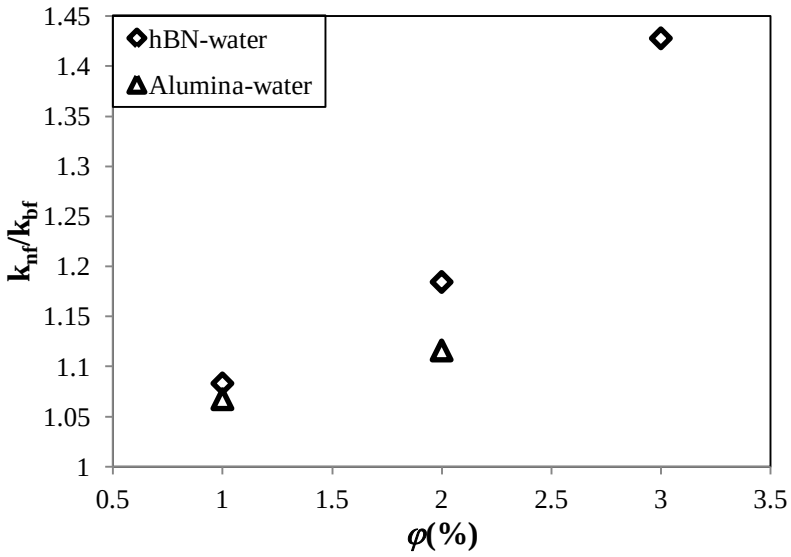

Figure 3.12. Comparison of thermal conductivity of pH adjusted Al_2O_3-water and hBN-water nanofluids.

3.4. hBN Nanofluids with Surfactants

In the preparation process of hBN-water nanofluids with 0.5, 0.75 and 1% volume concentrations, pH control has been employed in order to obtain stability. Although, the measured zeta potential values for diluted hBN-water nanofluids are high enough to indicate stability (see Figure 3.8) just after preparation, it is observed that sedimentation occurs within the nanofluids and after 1 or 2 days, significant sedimentation is observed

within prepared nanofluids. In order to solve the stability problem surfactant addition is employed for hBN-water nanofluids. GA and SDS are used in the experiments carried out with surfactants.

In surfactant addition process, nanofluid preparation procedure is employed accordingly: Desired amount of surfactant is added to the base fluid by using mechanical homogenizer. After mechanical homogenizer, surfactant-base fluid suspension is sonicated until it becomes transparent. In Figure 3.13, images of 3% GA by weight-water suspension (a) and homogeneous solution (b), before and after sonication are given accordingly. There is a significant difference in volume which can be clearly observed from the images. This difference is due to the density of foam before and after sonication. During sonication particles within the foam is dispersed into water, and foam becomes less dense after sonication. After the preparation of surfactant-base fluid solution, desired amount of hBN nanoparticles are weighed and suspended in the solution while it is mixing with mechanical homogenizer. After this procedure hBN suspensions are sonicated long enough to obtain stability. This preparation procedure is employed for both GA and SDS suspensions.

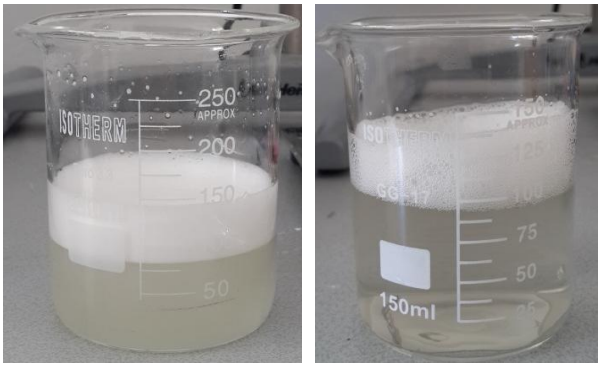

(a) (b)

Figure 3.13. 3% weight concentrated GA-water suspension and homogeneous solution, before (a) and after (b) sonication.

3.4.1. GA Addition to hBN Nanofluids

GA is an organic compound which is mainly used in food industry as a stabilizer. It has several other application areas such as printing, paint production, glue, cosmetics, and in viscosity control of fluids such as inks and textile products etc. In this study, GA is used to stabilize water, EG, and 50% water-50% EG based hBN nanofluids.

3.4.1.1. Preparation and Stability of hBN Nanofluids with GA Addition. The experimental procedure for surfactant addition is employed for hBN nanofluids as described in Table 3.5. After experimenting with several other GA concentrations, 5% GA by weight is found to give the most stable nanofluids. Sequential imaging method is used to observe the stability duration of hBN nanofluids as presented in Table 3.6.

Table 3.5. Preparation method for different hBN nanofluids.

Nanofluid	Particle Size [nm]	φ [%]	Sonication Time [hr]	Surfactant	Surfactant Concentration [%]
hBN-water	70	1	1	GA	5
hBN-water		2	1.5	GA	5
hBN-water		3	2	GA	5
hBN-water	70	1	1	SDS	0.1
hBN-water		2	1.5	SDS	0.1
hBN-water		3	1.5	SDS	0.1
hBN-EG	70	1	1	GA	5
hBN-EG		2	1.5	GA	5
hBN-EG		3	2	GA	7.5
hBN-water-EG	70	1	1	GA	5
hBN-water-EG		2	1.5	GA	5
hBN-water-EG		3	1.5	GA	5

A sequential image capturing study is employed for hBN-water nanofluids with 1% hBN by volume and 5% GA by weight. The images are presented in Figure 3.14. For this nanofluid particle and GA concentration, it is clearly seen that discoloration and layering begin after 12 days (Figure 3.14c). After 15 days, sedimentation is completed and hBN nanoparticles are collected at the bottom of the tube for this sample.

Table 3.6. Stability duration for hBN nanofluids with 5% weight concentrated GA addition.

Nanofluid	GA Concentration [%]	Stability Duration [day]
1% hBN-water	5	9
2% hBN-water	5	6
3% hBN-water	5	3
1% hBN-EG	5	1.5
2% hBN-EG	5	16
3% hBN-EG	5	6
1% hBN-50%water/EG	5	20
2% hBN-50%water/EG	5	17
3% hBN-50%water/EG	5	7

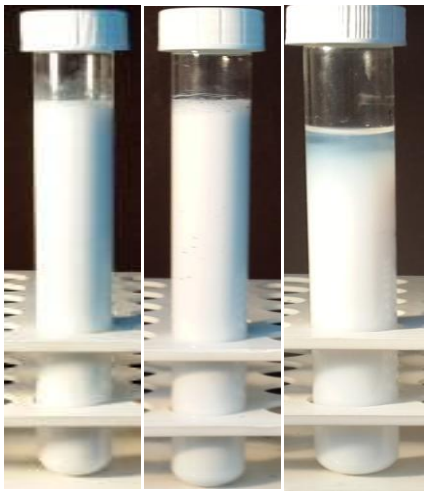

(a) (b) (c)

Figure 3.14. Sequential image capturing study for 1% volume concentrated hBN water nanofluids with the GA addition of 5% weight concentration, (a) 1 day, (b) 6 days, (c) 12 days.

3.4.1.2. Rheological Behavior of hBN Nanofluids with GA Addition. In determining the weight concentration of GA required for the most stable hBN nanofluids, viscosities of the samples are measured. In the viscosity investigation of 1% hBN-water nanofluids with the addition of GA at different weight concentrations, it is observed that the rheological behavior for all nanofluids is found to be Newtonian as it can be observed in Figure 3.15. However, the viscosity increases in these nanofluids are abnormally high; even for 2% GA weight concentration the viscosity increases to ~1.3 from ~0.89 mPas. This viscosity increase can also be observed in Figure 3.16. The viscosity values of DI water within same shear rate range is presented along with the nanofluid samples as well. While the viscosity increase with respect to the base fluid for 2% GA weight concentration is ~52%, it becomes ~%108 for 4% GA weight concentration. This data is the evidence that GA addition to the base fluid creates a viscosity increase that can surpass the thermal enhancement benefit acquired due to the nanoparticle addition. Viscosity value for 5% GA by weight concentration cannot be obtained due to this viscosity increase. The viscosity of 1% hBN water samples with 5% GA by weight concentration exceeds the limits of the rheometer. In order to overcome this viscosity increase problem with GA addition, SDS is considered as an alternative solution.

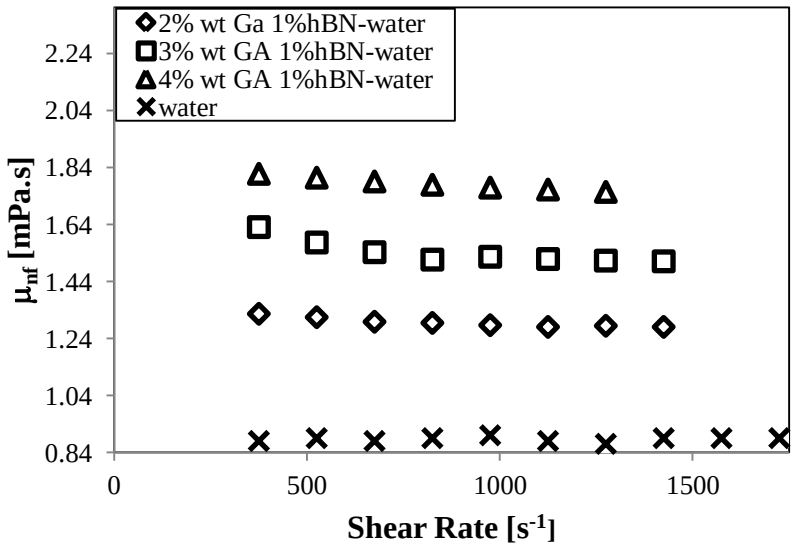

Figure 3.15. The viscosity of hBN nanofluids with 1% volume concentration for different %GA by weight changing within the shear rate range of 375-1425 s^{-1}.

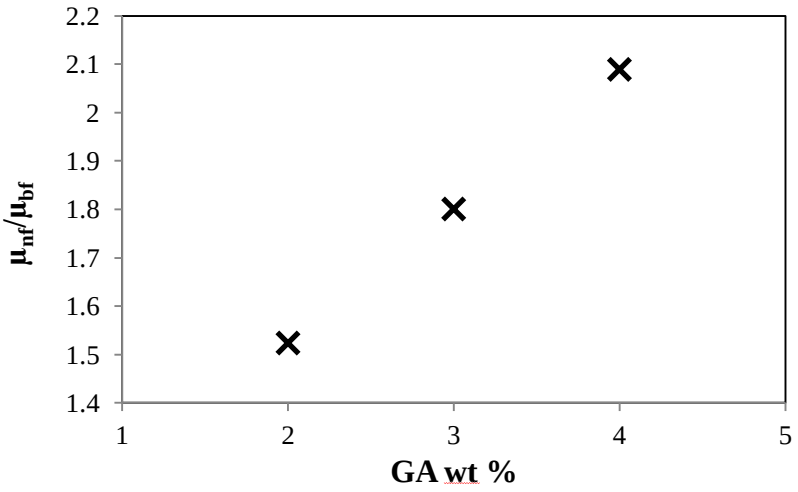

Figure 3.16. Viscosity ratio for hBN-water nanofluids with 1% volume concentration for different %GA by weight.

3.4.1.3. Thermal Conductivity Measurements of hBN Nanofluids with GA Addition. After the preparation of hBN nanofluids with 5% GA by weight concentration, their thermal conductivities are measured as presented in Figure 3.17. The best thermal enhancement for this data set can be obtained for hBN-50% water-EG nanofluids. For GA added hBN-water nanofluids, thermal enhancement is very poor compared to the one for pH adjusted hBN-water nanofluids. Furthermore, the thermal conductivity ratio of hBN-water and hBN-EG nanofluids exhibit similar behavior according to the same plot. GA addition with 5% weight concentration to the hBN nanofluids creates abnormal increase in viscosity that limits thermal conductivity enhancement. Since these nanofluids are considered as candidates of heat transfer fluid, nanofluids with higher thermal conductivity and lower viscosity should be obtained. As a solution of this problem, an alternative surfactant must be sought.

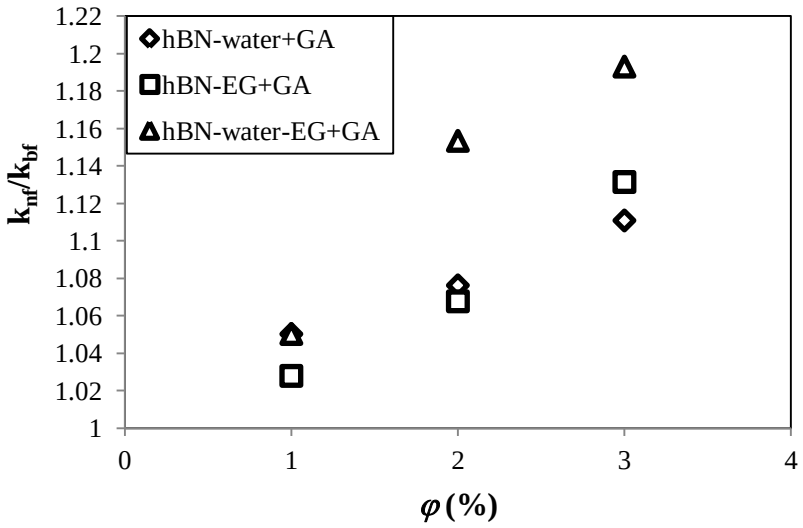

Figure 3.17. Thermal conductivity ratio vs. volume concentration of hBN nanofluids.

3.4.2. SDS Addition to hBN Nanofluids

The same preparation procedure is applied for the hBN-water nanofluids with SDS addition as well. The preparation method for these nanofluids is presented in Table 3.7. The weight concentration of SDS for hBN nanofluids to acquire stability is chosen to be 0.1%. A comparison of the molarities of hBN and SDS within 100 ml samples are presented in Table 3.8. The critical micelle concentration for SDS is 8×10^{-3} mol/L. Although, SDS molarities are not enough to form micelles within nanofluids, more SDS addition is not desirable as it increases viscosity and limits thermal conductivity enhancement. It is highly likely that SDS is forming a protective layer around the nanoparticles which reduces agglomeration. Stability duration of prepared hBN nanofluids with %0.1 SDS by weight addition is presented for different hBN volume concentrations in Table 3.9.

Table 3.7. Preparation method for hBN-water nanofluids with %SDS by weight addition.

Nanofluid	Particle Size [nm]	φ [%]	Sonic. Time [hr]	%SDS by wt.
hBN-water	70	1	1	0.10%
hBN-water	70	2	1	0.10%
hBN-water	70	3	1.5	0.10%

Table 3.8. Molarities of hBN and SDS within hBN-water nanofluids

φ [%]	SDS [mol/L]	hBN [mol/L]
1	3.55×10^{-3}	0.922
2	3.63×10^{-3}	1.845
3	3.71×10^{-3}	2.767

Table 3.9. Stability duration for hBN nanofluids with %SDS by weight addition.

Nanofluid	φ [%]	Surfactant	Surf. Conc. [%]	Stability [day]
hBN-water	1	SDS	0.1	6
hBN-water+EG	2	SDS	0.1	5
hBN-water+EG	3	SDS	0.1	3

The main reason for choosing SDS instead of GA as a surfactant is the significant viscosity increase that limits the thermal enhancement. As a result, the overall heat transfer performance of nanofluids could be negatively affected. Thus, viscosity of hBN nanofluids with SDS addition is checked first.

Viscosity measurements within the shear rate range of 375-1687.5 s^{-1} for different volume concentrations (1, 2, 3%) of hBN nanofluids with SDS addition is presented in Figure 3.18. It can be clearly seen that for 1% hBN-water nanofluids with SDS additives the viscosity is almost the same as the viscosity of water. Viscosity increase with increasing particle volume concentration is milder than that is for GA addition for SDS added nanofluids. Viscosity of 1% hBN-water with the addition of 2% GA by weight is ~1.3 mPa.s, whereas

1% hBN-water with the addition of 0.1% SDS by weight has a viscosity value of ~0.9 mPa.s. It can be concluded that stable hBN-water nanofluids can be prepared by using smaller amounts of SDS that leads to relatively less increase in viscosity. Furhermore, for hBN nanofluids with 0.1% SDS by weight, 1, 2, 3% particle volume concentrations are all exhibited Newtonian behavior within the shear rate range of 375-1687.5 s^{-1}.

In Figure 3.19, the viscosity of hBN-water nanofluids with SDS addition and pH control, and Al_2O_3-water nanofluids are compared for different volume concentrations. It is clearly seen that hBN nanofluids have lower viscosity increase than the one for Al_2O_3-water nanofluids with respect to the base fluid viscosity. As it is expected, surfactant addition creates higher viscosity increase than the one without any surfactant if the viscosity ratio of hBN-water nanofluids with SDS addition and pH control are compared. It should be noted that addition of 0.1% SDS by weight to the base fluid leads to negligible difference in base fluid viscosity.

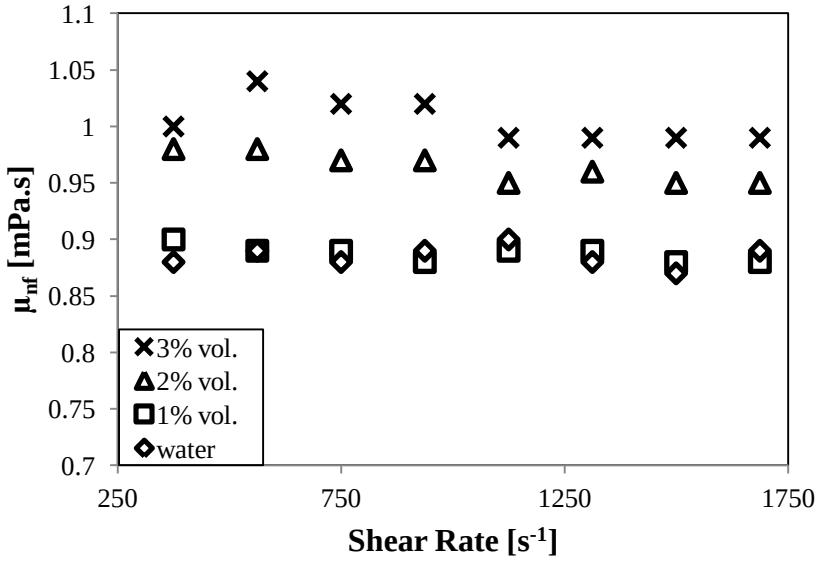

Figure 3.18. Viscosity of hBN-water nanofluids with %SDS by weight concentration and different hBN volume concentrations presented in Table 3.7 in the shear rate range of 375-1687.5 s^{-1}.

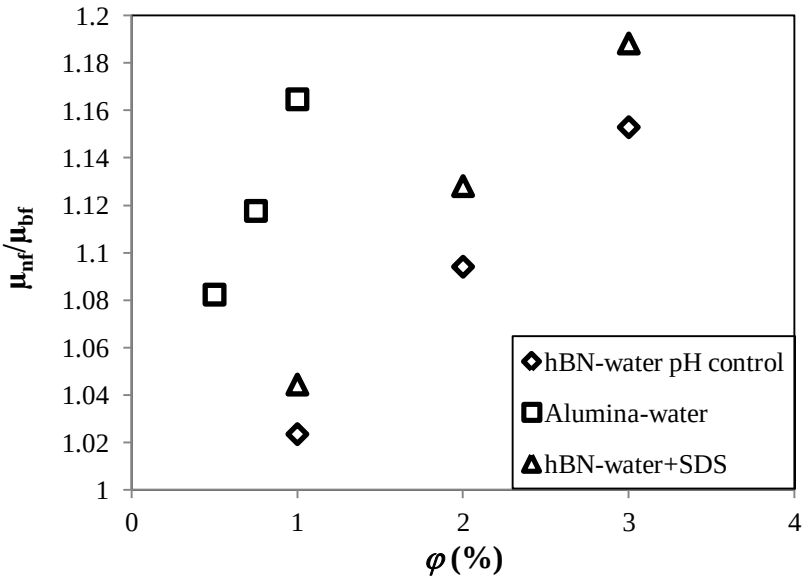

Figure 3.19. Comparison of viscosity change of hBN water nanofluids with SDS addition and pH control, and Al_2O_3-water nanofluids for different volume concentrations.

In Figure 3.20, hBN nanofluid thermal conductivity ratio with respect to the base fluids for different volume concentrations are presented. hBN-water nanofluids prepared with pH control have the highest thermal conductivity enhancement compared to other hBN nanofluids, but as it is reported before they are not stable for longer periods of time.

On the other hand, hBN nanofluids with SDS addition are stable for longer periods and have a thermal conductivity enhancement of ~29% exceeding the enhancement observed with GA addition that is ~20% for 3% particle volume concentration. It can be concluded that from this result SDS is a superior surfactant than GA for hBN-water nanofluids when stability, thermal and rheological performance are considered.

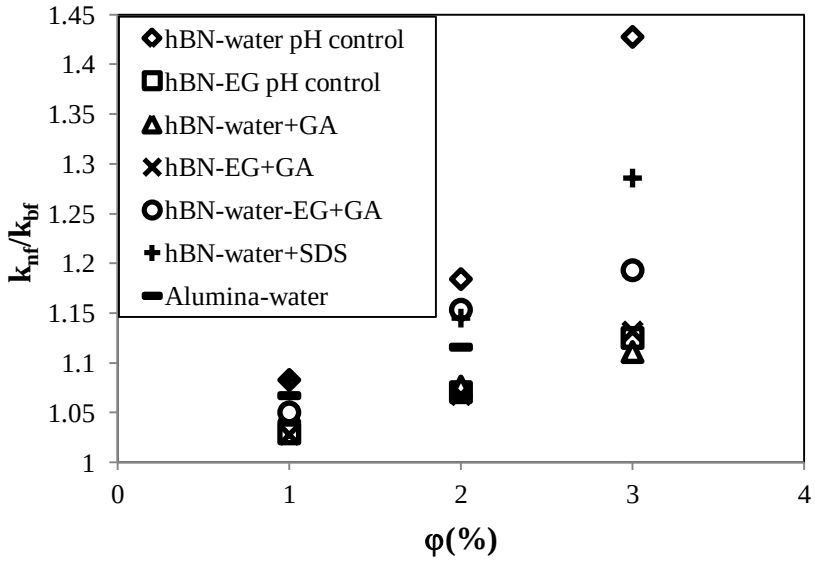

Figure 3.20. Comparison of thermal conductivity ratio of hBN nanofluids prepared for this study.

3.5. Validation of Convective Heat transfer Test Setup with Water

After the construction of convective heat transfer test setup it is calibrated with water. In this experiment, heat flux applied to the tube is ~453 W and the Reynolds number is 1805. It can be seen from Figure 3.21 that the convection test setup produces similar results with the theoretical data calculated from Shah correlation. An uncertainty analysis is performed as it is presented in previous chapter. Measured local heat transfer coefficients and local Nu for water along the pipe are presented with the measurement error bars which is compared with the data obtained from Shah correlation as it can be observed in Figure 3.22 and Figure 3.23 respectively. Measured values are in the error range if they are compared with the theoretical values calculated from Shah correlation.

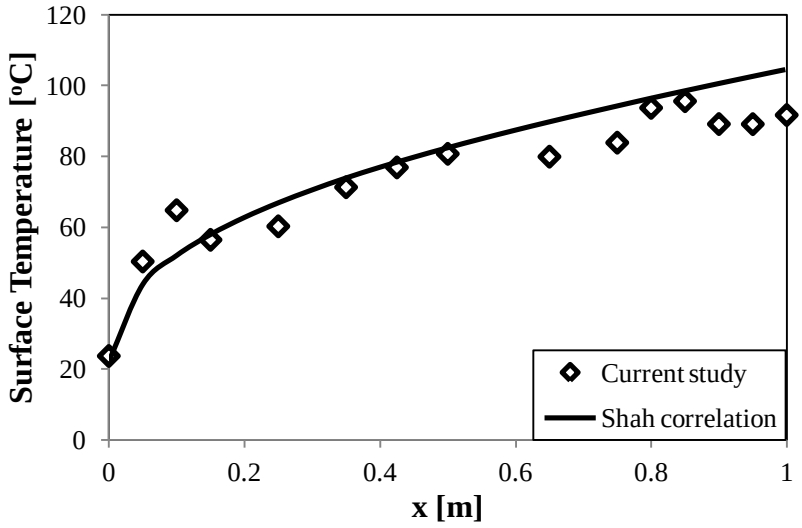

Figure 3.21. Measured surface temperature values along the test tube comparing with the values calculated from Shah correlation.

The measurement error in h_x and Nu_x is in the range of 30-40% of the measured value according to the uncertainty analysis. Therefore, this high measurement uncertainty is needed to be minimized. If the heat section has poor insulation the heat produced by the resistance cannot be fully transferred to water. It should be calculated by using measured inlet and outlet temperature values, and flow rate as in the present study. As a result, an error is introduced because of these measured values. If the heat transferred to water is known, there is no need to calculate it and no error to be introduced. In Figure 3.24, relative uncertainty in Nu_x is presented for the calculated and known q cases. There is a big difference in uncertainty between two cases. From this figure, it can be inferred that the uncertainty in measured Nu_x and h_x is mostly depends on the measurement uncertainty in q. Therefore, better insulation is needed along the pipe to minimize measurement error in local heat transfer coefficient and Nusselt number.

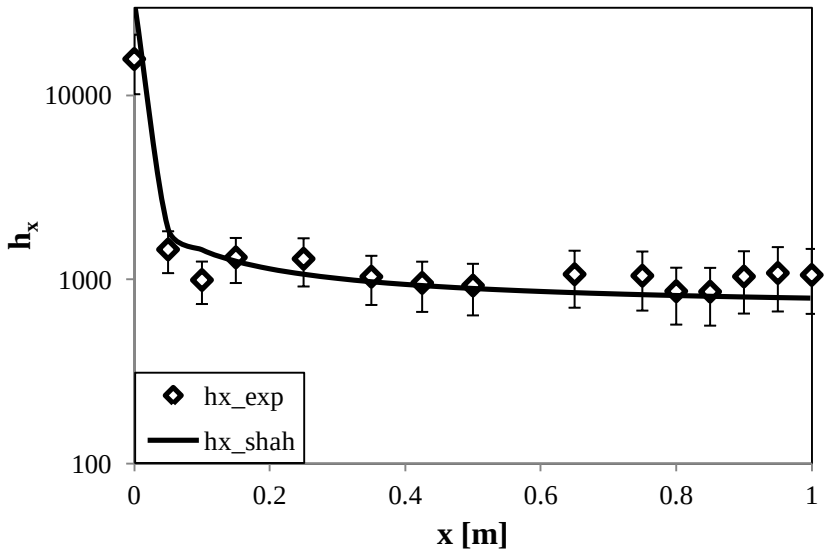

Figure 3.22. Local heat transfer coefficients measured and calculated from Shah correlation along the pipe with measurement error bars.

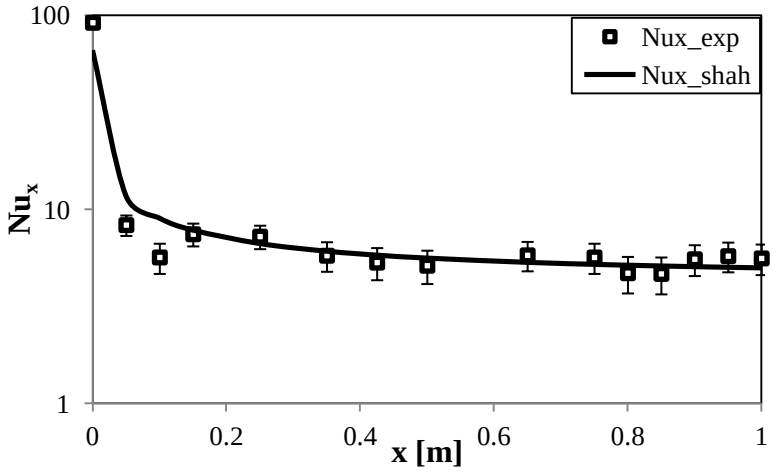

Figure 3.23. Local Nusselt numbers measured and calculated from Shah correlation along the pipe with measurement error bars.

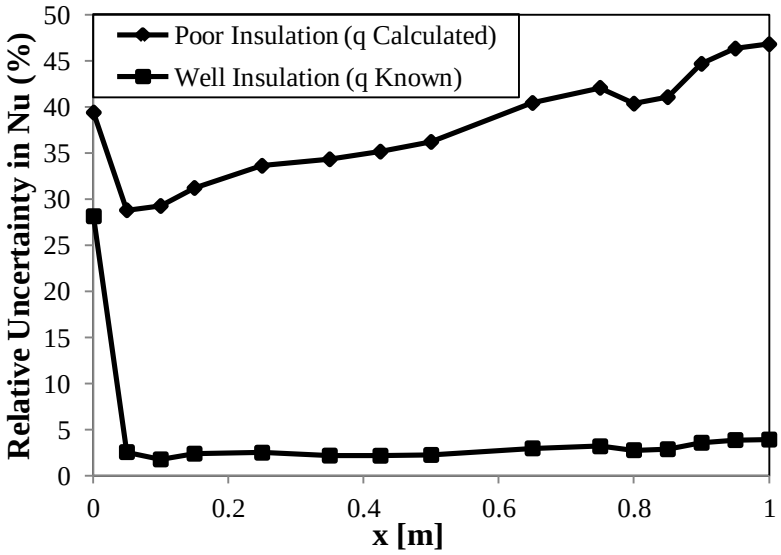

Figure 3.24. Comparison of % relative uncertainty in Nu for well insulated and poor insulated (present setup) heating section.

4. CONCLUSION AND RECOMMENDATIONS FOR FUTURE WORK

4.1. Conclusion

Nanofluids are proposed as next generation heat transfer fluids due to their superior thermal behaviors. Since hexagonal BN has a superior chemical stability and thermal conductivity, preparation of stable hBN nanofluids and characterization of their thermal and rheological behaviors are the objectives of this study. Furthermore, the construction of a convective heat transfer test setup to investigate enhancement in local heat transfer coefficient of nanofluids is executed and the test setup is validated by DI water.

In order to provide stable dispersions, parameters such as sonication time, pH of the base fluid, surfactant type and concentration are examined for hBN nanofluids. A validation study for 15 nm γ-Al_2O_3-water nanofluids is executed and the measured values are found to be in a good agreement with the literature (Lai, 2010). In the pH study the preparation procedure is optimized by considering former agglomeration level of dry nanoparticles, and the stability and sedimentation status within dispersions after preparation. The optimum sonication time is found to be as 3 hours and the optimum pH levels are determined as 12 for hBN-water nanofluids of 0.5% particle volume concentration. Optimized pH and sonication time is changing with the change in particle volume concentration. Therefore, similar optimization studies for other particle volume concentrations are employed and the optimum pH levels are determined either as 9 or 12 for 0.75 and 1% volume concentrations respectively. In this procedure no surfactant additive is used. However, although their zeta potential indicate good level of stability just after the preparation, pH adjusted hBN nanofluids are not stable for long time periods. Therefore, surfactant addition method is employed to achieve more stable hBN nanofluids.

First, GA is used as a surfactant. 5% GA by weight is determined to be the ideal concentration for preparing stable hBN nanofluids. In this study water, EG and 50% water-50% EG are used as base fluids. For 50% water-50% EG based hBN nanofluids of 1% particle volume concentration, stability duration time is up to 20 days using 5% GA by weight. However, the viscosity increase of hBN-water nanofluids using 2, 3, 4% GA by weight is observed to be significant, that also suppresses the thermal conductivity enhancement. Therefore, SDS is sought as an alternative solution. Addition of 0.1% SDS by weight improves stability of hBN-water nanofluids while the increase in viscosity is relatively smaller than that for corresponding cases with GA addition. Besides, thermal conductivity enhancement is remarkably higher than that is for GA addition. Therefore, SDS can be considered as a better surfactant material for hBN-water nanofluids than GA, considering their thermal and rheological performance.

All the tested nanofluids exhibit Newtonian behavior within the shear rate range of 150-2000 s^{-1}. The lowest viscosity increase and the highest thermal conductivity enhancement can be obtained for pH adjusted hBN nanofluids. However they are not stable for long time periods. On the other hand, hBN nanofluids with SDS addition have better stability and have a thermal conductivity enhancement exceeding the one for GA addition. Furthermore, hBN-water nanofluids with SDS addition have remarkably lower viscosity increase than the one for GA addition.

Furthermore, a test setup to investigate convective heat transfer behavior of nanofluids is constructed and validated through experiments carried out with water. A measurement uncertainty analysis is conducted and it is presented with the obtained local heat transfer coefficients by comparing them with the trend obtained from Shah correlation. It can be concluded that the test setup produces acceptable data for water within the presented measurement uncertainty range.

4.2. Recommendations for Future Work

Following this study, convective heat transfer behavior of the presented hBN nanofluids should be carried out with the constructed test setup to investigate the enhancement in local heat transfer coefficient of nanofluids. The insulation along the heat section of the test setup should be improved in order to minimize the measurement uncertainty.

Different preparation recipes can be proposed to enable better stability for hBN nanofluids. Further investigation with hBN nanofluids by using SDS or different type of surfactants might be carried out in this regard. In this study, SDS was used with a weight concentration of 0.01%, different experiments can be conducted with more amount of SDS addition. As it was observed with GA addition, surfactant addition introduces further viscosity increase to the nanofluids. Different anionic surfactants can be proposed to minimize this effect. The combination of pH control and surfactant addition might be preferred as an alternative solution to viscosity increase problem. In the pH study with hBN-water nanofluids, pH between 7 and 9 for 0.001% diluted samples give higher zeta potential values. Further investigation can be carried out within this pH range.

In this study, experiments of viscosity and thermal conductivity measurements for hBN nanofluids were conducted with 1,2, and 3% hBN by volume. Higher volume concentrations can be preferred in order to determine the overall heat transfer performance of hBN nanofluids as heat transfer fluids. Moreover, temperature dependency of viscosity and thermal conductivity might be another focus in the investigation of nanofluids' thermal properties.

APPENDIX A: ZETA POTENTIAL EXPERIMENTS

Table A.1. Zeta potential measurement for hBN-water nanofluid at 0.5% volume concentration at pH 6 for 1 hour sonication and 0.001% dilution.

Run	Mobility	Zeta Potential [mV]	Rel. Residual
1	-1.97	-25.24	0.0343
2	-2.17	-27.8	0.0083
3	-2.26	-28.92	0.0138
4	-2.16	-27.61	0.0142
5	-1.78	-22.76	0.0228
6	-2.17	-27.83	0.0276
7	-2.41	-30.85	0.009
8	-2.43	-31.06	0.0114
9	-2.18	-27.93	0.0159
10	-1.98	-25.33	0.0179
Mean	-2.15	-27.53	0.0175
Std. Error	0.06	0.91	0.0027
Combined	-2.15	-27.56	0.0075

Table A.2. Zeta potential measurement for hBN-water nanofluid at 0.5% volume concentration at pH 6 for 1.5 hour sonication and 0.001% dilution.

Run	Mobility	Zeta Potential [mV]	Rel. Residual
1	-2.01	-25.78	0.0268
2	-2.2	-28.17	0.0152
3	-1.95	-25	0.0254
4	-1.81	-23.19	0.0213
5	-1.27	-16.29	0.0282
6	-0.97	-12.41	0.0401
7	-1.02	-13.04	0.0384
8	-1.26	-16.15	0.026
9	-1.54	-19.67	0.029
10	-2.35	-30.05	0.0106
Mean	-1.64	-20.97	0.0261
Combined	-1.63	-20.84	0.0079

APPENDIX B: EFFECTIVE AGGREGATE SIZE MEASUREMENTS

1. hBN-water sample, 0.5% volume concentration, 2 hr sonication, pH 9 (Combined)

Effective Diameter: 351.6

Polydispersity: 0.205

Baseline Index: 7.5/ 54.16%

Elapsed Time = 00:08:00

Table B.1. Aggregate size measurement for hBN- water nanofluid with 0.5% hBN by volume at pH 9 (base fluid) and for 2 hour sonication.

Run	Eff. Diam. [nm]	Half Width [nm]	Polydispersity	Baseline Index
1	338.6	169.7	0.251	4.1/ 54.22%
2	366.1	168.6	0.212	8.5/ 64.00%
3 (inactive)	352.6	61.3	0.03	3.9/ 53.78%
4	357.3	176.4	0.244	7.7/ 48.44%
5 (inactive)	542.3	475.7	0.769	0.0/ 3.56%
6	371.2	173.5	0.218	8.4/ 41.33%
7	357.3	167.3	0.219	9.7/ 72.12%
8	345.2	161.3	0.218	6.4/ 53.78%
9	345	102.4	0.088	3.2/ 60.89%
10	328.7	152.9	0.216	4.4/ 38.50%
Mean	351.2	159	0.208	6.6/ 54.16%
Std.Error	5.1	8.5	0.018	0.8/ 4.03
Combined	351.6	159.3	0.205	7.5/ 54.16%

2. hBN-water sample, %0.5 volume concentration, 2 hr sonication, pH 11 (Combined)

Effective Diameter: 327.3

Polydispersity: 0.166

Baseline Index: 8.1/ 54.38%

Elapsed Time = 00:08:00

Table B.2. Aggregate size measurement for hBN- water nanofluid with 0.5% hBN by volume at pH 11 (base fluid) and for 2 hour sonication.

Run	Eff. Diam. [nm]	Half Width [nm]	Polydispersity	Baseline Index
1 (inactive)	329.3	143.3	0.189	1.0/ 57.78%
2	320.6	139.3	0.189	5.0/ 65.49%
3	317	110.8	0.122	5.3/ 58.22%
4	322.9	161.2	0.249	8.5/ 60.89%
5	335.7	118.1	0.124	8.9/ 58.67%
6	339.6	162	0.228	7.8/ 58.41%
7	320.3	134.5	0.176	5.6/ 45.33%
8 (inactive)	306.6	93.4	0.093	0.5/ 28.00%
9	329.6	133.4	0.164	7.4/ 62.67%
10	337.5	60.2	0.032	6.3/ 25.33%
Mean	327.9	127.4	0.16	6.8/ 54.38%
Std.Error	3.1	11.5	0.024	0.5/ 4.65
Combined	327.3	133.4	0.166	8.1/ 54.38%

APPENDIX C: STABILITY INSPECTION IMAGES

1. EG - 1% vol. hBN - 5% wt SDS

(a) (b)

Figure C.1. hBN-EG nanofluid samples with 1% hBN by volume and 5% SDS by volume after 15 minutes (a), and 1 hour (b).

2. Water - 3% vol. hBN-5% wt GA

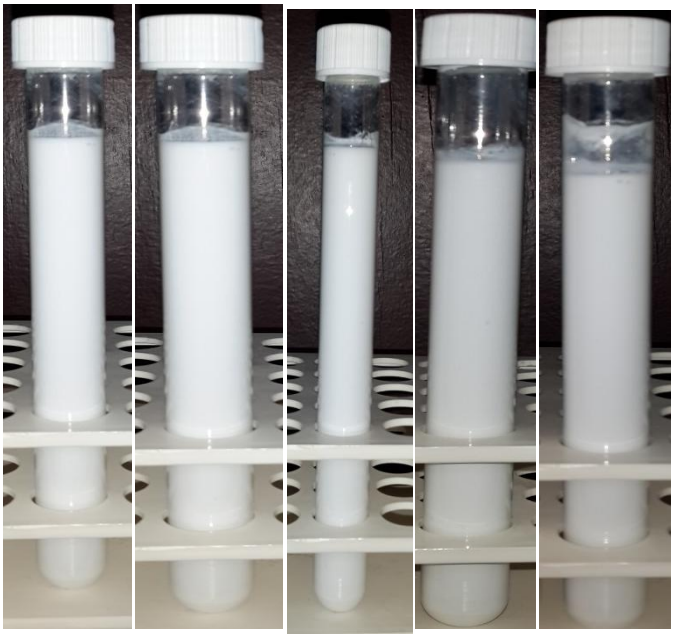

(a) (b) (c) (d) (e)

Figure C.2. hBN-water nanofluid samples with 3% hBN by volume and 5% GA by weight after 1hr (a), 1 day (b), 1.5 day (c), 2 days (d), and 3 days (e).

3. Water - 1% vol. hBN-5% wt. GA

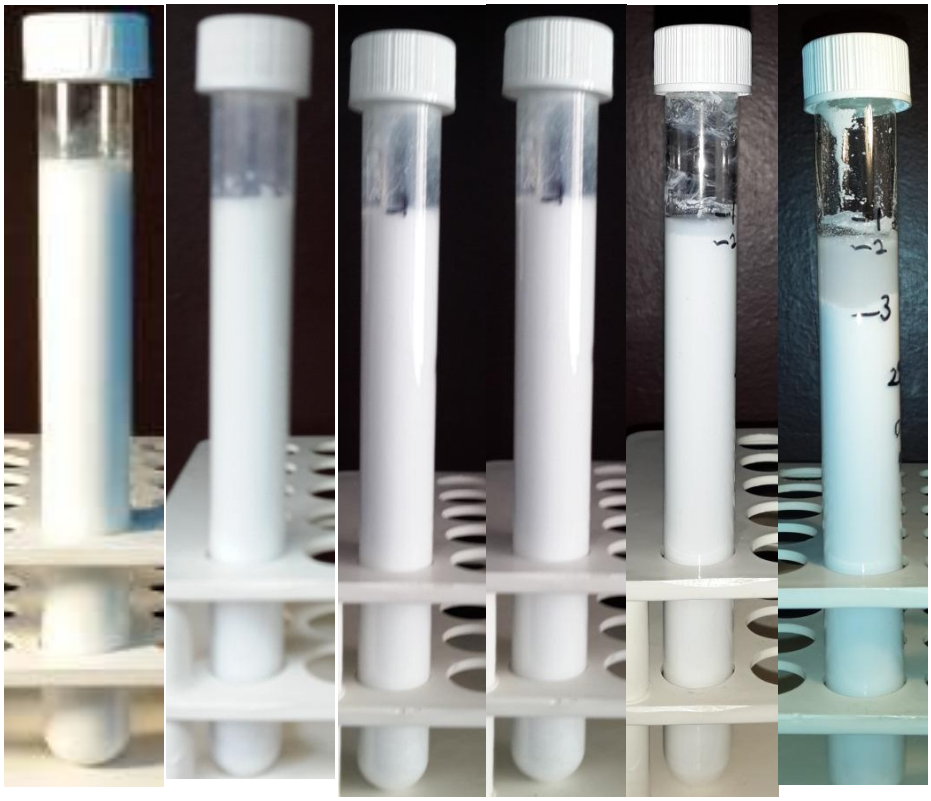

Figure C.3. hBN-water nanofluid sample with 1% hBN by volume and 5% GA by weight after 1 day (a), 6 days (b), 7 days (c), 9 days (d), and 10.5 days (e), and 11 days (f).

4. Water+EG - 2% vol. hBN-5% wt GA

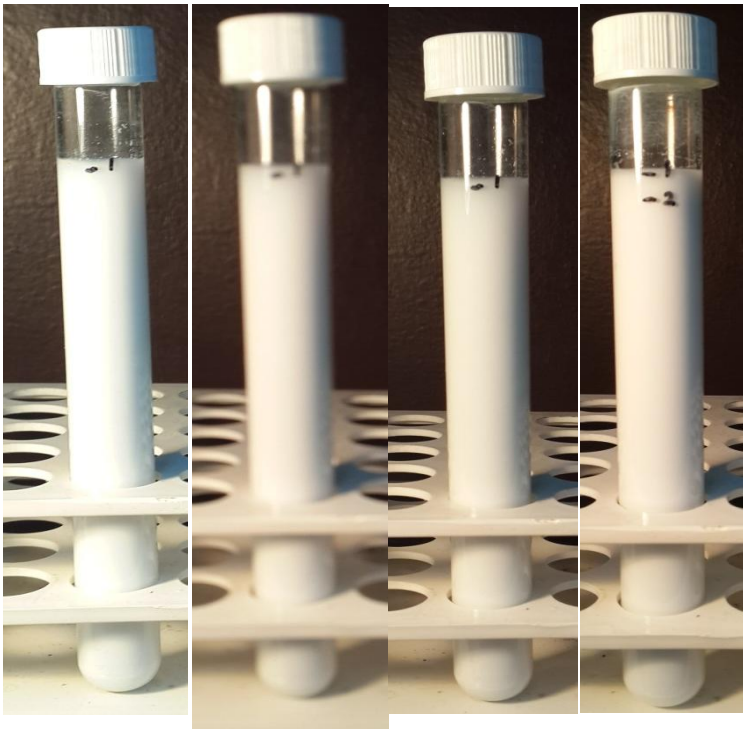

(a) (b) (c) (d)

Figure C.4. hBN 50%water-EG nanofluid sample with 2% hBN by volume and 5% GA by weight after 1 day (a), 6 days (b), 12 days (c), and 16 days (d).

REFERENCES

Anoop, K. B., S. Kabelac, T. Sundararajan, S. K. Das, 2009, "Rheological and Flow Characteristics of Nanofluids: Influence of Electroviscous Effects and Particle Agglomeration", *Journal of Applied Physics*, Vol. 106, No. 3.

Batchelor, G.K., 1977, "The Effect of Brownian Motion on the Bulk Stress In A Suspension of Spherical Particles", *Journal of Fluid Mechanics*, Vol. 83, No. 1, pp. 97-117.

Beck, M. P., Y. H. Yuan, P. Warrier, A. S. Teja, 2009, "The Effect of Particle Size On The Thermal Conductivity of Alumina Nanofluids", *Journal of Nanoparticle Research*, Vol. 11, No. 5, pp. 1129-1136.

Bird R. B., R. C. Armstrong, O. Hassager, 1987, *Dynamics of Polymeric Liquids. Vol I*, 2nd edition, Wiley, New York.

Brinkman H. C., 1947, "A Calculation of the Viscous Force Exerted By A Flowing Fluid on A Dense Swarm Of Particles", *Journal of Applied Sciences Research*, Vol. 1, No. 1, pp. 27-34.

Brookfield Rheometer Manuals, *Brookfield Digital Rheometer Model DV-III Operating Instructions*, http://www.brookfieldengineering.com/download/files/DV3.pdf, [Accessed February 2012].

Bruggeman, D. A. G., 1935, "Berechnung Verschiedener Physikalischer Konstanten von Heterogenen Substanzen, I. Dielektrizitatskonstanten und Leitfahigkeiten Der Mischkorper aus Isotropen Substanzen", *Annalen der Physik*, Vol. 24, pp. 636-679.

Buongiorno, J., D. C. Venerus, N. Prabhat, T. McKrell, J. Townsend, R. Christianson, Y. V. Tolmachev, P. Keblinski, L.-w Hu, J. L. Alvarado, I. C. Bang, S. W. Bishnoi, M. Bonetti, F. Botz, A. Cecere, Y. Chang, G. Chen, H. Chen, S. J. Chung, M. K. Chyu, S. K. Das, R. D.

Paola, Y. Ding, F. Dubois, G. Dzido, J. Eapen, W. Escher, D. Funfschilling, Q. Galand, J. Gao, P. E. Gharagozloo, K. E. Goodson, J. G. Gutierrez, H. Hong, M. Horton, K. S. Hwang, C. S. Iorio, S. P. Jang, A. B. Jarzebski, Y. Jiang, L. G. Kieng, C. Kim, J. H. Kim, S. Kim, S. H. Lee, J. Phillip, D. Poulikakos, C. Reynaud, R. Savino, P. K. Singh, P. Song, T. Sundararajan, E. Timofeeva, T. Tritcak, A. N. Turanov, S. V. Vaerenbergh, D. Wen, S. Witharana, C. Yang, W.-H. Yeh, X.-Z. Zhao, S.-Q., Zhou, 2009, "A Benchmark Study On the Thermal Conductivity of Nanofluids", *Journal of Applied Physics*, Vol. 106, No. 9.

Carslaw, H. S. and Jaeger, J. C., 1959, *Conduction of Heat in Solids*, 2nd edition, Oxford: Clarendon Press.

Chandrasekar, M., S. Suresh, A. C. Bose, 2010, "Experimental Investigations and Theoretical Determination of Thermal Conductivity and Viscosity of Al_2O_3/Water Nanofluid", *Journal of Experimental Thermal and Fluid Science*, Vol. 34, No. 2, pp. 210-216.

Chen H., S. Witharana, Y. Jin, C. Kim, Y. Ding, 2009, "Predicting Thermal Conductivity of Liquid Suspensions of Nanoparticles (Nanofluids) Based On Rheology", *Journal of Particuology*, Vol. 7, No. 2, pp. 151-157.

Chen, G., W. Yu, D. Singh, D. Cookson, J. Routbot, 2008, "Application of SAXS to the Study of Particle-Size-Dependent Thermal Conductivity in Silica Nanofluids", *Journal of Nanoparticle Research*, Vol. 10, No. 7, pp. 1109-1114.

Choi, S. U. S., 1995, "Enhancing Thermal Conductivity of Fluids with Nanoparticles", *Developments and Applications of Non-Newtonian Flows*, ASME, New York, pp. 99–105.

Chon, C. H., K. D. Kihm, S. P. Li, S. U. S. Choi, 2005, "Empirical Correlation Finding the Role of Temperature And Particle Size for Nanofluid (Al_2O_3) Thermal Conductivity Enhancement", *Journal of Applied Physics Letters*, Vol. 87, No. 15.

Chopkar, M., P. K. Das, I. Manna, 2006, "Synthesis and Characterization of Nanofluid for Advanced Heat Transfer Applications", *Indranil Scripta Materialia*, Vol. 55, No. 6, pp. 549-552.

Chou, J. C., L. P. Liao, 2005, "Study On pH at the Point of Zero Charge of TiO_2 pH Ion-Sensitive Field Effect Transistor Made by the Sputtering Method", *Thin Solid Films*, Vol. 476, No. 1, pp. 157-161.

Colla, L., L. Fedele, M. Scattolini, S. Bobbo, 2012, "Water-Based Fe_2O_3 Nanofluid Characterization: Thermal Conductivity and Viscosity Measurements and Correlation", *Advances in Mechanical Engineering*.

Das, S. K., N. Putra, P. Thiesen, W. Roetzel, 2003, "Temperature Dependence of Thermal Conductivity Enhancement for Nanofluids", *Journal of Heat Transfer-Transactions of the ASME*, Vol. 125, No. 4, pp. 567-574.

Das, S. K., N. Putra, W. Roetzel, 2003, "Pool Boiling of Nanofluids On Horizontal Narrow Tubes", *International Journal of Multiphase Flow*, Vol. 29, No. 8, pp. 1237-1247.

Ding Y., H. Alias, D. Wen, R. A. Williams, 2006, "Heat Transfer of Aqueous Suspensions of Carbon Nanotubes (CNT Nanofluids)", *International Journal of Heat and Mass Transfer*, Vol. 49, No. 1-2, pp. 240–250.

Ding, Y., H. Chen, Z. Musina, Y. Jin, T. Zhang, S. Witharana, W. Yang, 2010, "Relationship Between the Thermal Conductivity and Shear Viscosity of Nanofluids", *3rd International Symposium on Functional Materials/Advances in Functional Materials Conference*, Jinju City, South Korea, Vol. T139, June 15-18, 2009.

Eapen, J., J. Li, S. Yip, 2007, "Beyond the Maxwell Limit: Thermal Conduction In Nanofluids with Percolating Fluid Structures", *Physical Review E*, Vol. 76, No. 6.

Eapen, J., J. Li, S. Yip, 2007, "Mechanism of Thermal Transport In Dilute Nanocolloids", *Physical Review Letters*, Vol. 98, No. 2.

Eastman, J. A., S. U. S. Choi, S. Li, 2001, "Anomalously Increased Effective Thermal Conductivities of Ethylene Glycol-Based Nanofluids Containing Copper Nanoparticles", *Applied Physics Letters*, Vol. 78, No. 6, pp. 718-720.

Einstein, A., 1905, *Investigations on the Theory of the Brownian Movement*, Dover Publications, New York.

Fedele, L., L. Colla, S. Bobbo, S. Barison, F. Agresti, 2011, "Experimental Stability Analysis of Different Water-Based Nanofluids", *Nanoscale Research Letters*, Vol. 6.

Ghadimi, A., R. Saidur, H. S. C. Metselaar, 2011, "A Review of Nanofluid Stability Properties and Characterization in Stationary Conditions", *International Journal of Heat and Mass Transfer*, Vol. 54, No. 17-18, pp. 4051-4068.

Hamilton, R. L. and O. K. Crosser, 1962, "Thermal Conductivity of Heterogeneous Two-Component Systems", *Industrial and Engineering Chemistry Fundamentals*, Vol. 1, No. 3, pp. 187-191.

Hong, J. and D. Kim, 2012, "Effects of Aggregation on the Thermal Conductivity of Alumina/Water Nanofluids", *Thermochimica Acta*, Vol. 542, pp. 28-32.

Hong, T. K., H. S. Yang, C. J. Choi, 2005, "Study of the Enhanced Thermal Conductivity of Fe Nanofluids", *Journal of Applied Physics*, Vol. 97, No. 6.

Hong, K. S., T. K. Hong, H. S. Yang, 2006, "Thermal Conductivity of Fe Nanofluids Depending on the Cluster Size of Nanoparticles", *Applied Physics Letters*, Vol. 88, No. 3.

Huang, J., X. Wang, Q. Long, X. Wen, Y. Zhou, L. Li, 2009, "Influence of pH on the Stability Characteristics of Nanofluids", *Symposium on Photonics and Optoelectronics*, Wuhan, People R China, August 14-16, 2009, pp. 879-882.

Hwang, Y., J. K. Lee, C. H. Lee, Y. M. Jung, S. I. Cheong, C. G. Lee, B. C. Ku, S. P. Jang, 2007, "Stability and Thermal Conductivity Characteristics of Nanofluids", *Thermochimica Acta*, Vol. 455, No. 1-2, pp. 70-74.

Jang, S. P. and S. U. S. Choi, 2004, "Role of Brownian Motion in the Enhanced Thermal Conductivity of Nanofluids", *Applied Physics Letters*, Vol. 84, No. 21, pp. 4316-4318.

Jung, J. Y., H. S. Oh, H. Y. Kwak, 2009, "Forced Convective Heat Transfer of Nanofluids in Microchannels", *International Journal of Heat and Mass Transfer*, Vol. 52, pp. 466-472.

Kalyan C. S., 2008, *Development of Computerized Transient Hot-Wire Thermal Conductivity (HWTC) Apparatus for Nanofluids*, M.S. Thesis, Northern Illinois University.

Kang, H. U., S. H. Kim, J. M. Oh, 2006, "Estimation of Thermal Conductivity of Nanofluid Using Experimental Effective Particle Volume", *Journal of Experimental Heat Transfer*, Vol. 19, No. 3, pp. 181-191.

Keblinski, P., S. R. Phillpot, S. U. S. Choi, J. A. Eastman, 2002, "Mechanisms of Heat Flow in Suspensions of Nano-Sized Particles (Nanofluids)", *International Journal of Heat and Mass Transfer*, Vol. 45, No. 4, pp. 855-863.

Kim, S. H., S. R. Choi, D. Kim, 2007, "Thermal Conductivity of Metal-Oxide Nanofluids: Particle Size Dependence and Effect of Laser Irradiation", *Journal of Heat Transfer-Transactions of the ASME*, Vol. 129, No. 3, pp. 298-307.

Lai, W. Y., 2010, *Experiments on Laminar Convective Heat Transfer with gamma-Aluminum Oxide Nanofluids*, Ph.D. Thesis, Arizona State University.

Lee, D., J. W. Kim, B. G. Kim, 2006, "A New Parameter to Control Heat Transport in Nanofluids: Surface Charge State of The Particle in Suspension", *Journal of Physical Chemistry B*, Vol. 110, No. 9, pp. 4323-4328.

Li, C. H. and G. P. Peterson, 2006, "Experimental Investigation of Temperature and Volume Fraction Variations on The Effective Thermal Conductivity of Nanoparticle Suspensions (Nanofluids)", *Journal of Applied Physics*, Vol. 99, No. 8.

Li, C. H. and G. P. Peterson, 2007, "The Effect of Particle Size on the Effective Thermal Conductivity of Al_2O_3-Water Nanofluids", *Journal of Applied Physics*, Vol. 101, No. 4.

Li, Y., J.'e. Zhou, Z. Luo, S. Tung, E. Schneider, J. Wu, and X. Li, 2011, "Investigation on Two Abnormal Phenomena about Thermal Conductivity Enhancement of BN/EG Nanofluids", *Nanoscale Research Letters*, Vol. 6.

Li, Q. and Y. M. Xuan, 2000, "Experimental Investigation on Transport Properties of Nanofluids", *5th International Symposium on Heat Transfer*, Beijing, Peoples R China, August 12-16, 2000, Heat Transfer Science and Technology 2000.

Liu, D. and L. Y. Yu, 2011, "Single-Phase Thermal Transport of Nanofluids in a Minichannel", *Journal of Heat Transfer-Transactions of the ASME*, Vol. 133, No. 3.

Lundgren, T. S., 1972, "Slow Flow through Stationary Random Beds and Suspensions of Spheres" *Journal of Fluid Mechanics*, Vol. 51, pp. 273–299.

Maiga, S. E. B., C. T. Nguyen, N. Galanis, G. Roy, 2004, "Heat Transfer Behaviors of Nanofluids in a Uniformly Heated Tube", *Superlattices and Microstructures*, Vol. 35, No. 3-6, pp. 543-557.

Mallick, S. S., A. Mishra, L. Kundan, 2013, "An Investigation into Modelling Thermal Conductivity for Alumina-Water Nanofluids", *Powder Technology*, Vol. 233, pp. 234-244.

Maxwell, J. C., 1881, *A Treatise on Electricity and Magnetism*, 2nd edition, Clarendon, Oxford.

Murshed, S. M. S., K. C. Leong, C. Yang, 2005, "Enhanced Thermal Conductivity of TiO_2 - Water Based Nanofluids", *International Journal of Thermal Sciences*, Vol. 44, No. 4, pp. 367-373.

Mintsa, H. A., G. Roy, C. T. Nguyen, D. Doucet, 2009, "New Temperature Dependent Thermal Conductivity Data for Water-Based Nanofluids", *International Journal of Thermal Sciences*, Vol. 48, No. 2, pp. 363-371.

Nguyen, C. T., F. Desgranges, G. Roy, N. Galanis, T. Mare, S. Boucher, H. A. Mintsa, 2007, "Temperature and Particle-Size Dependent Viscosity Data for Water-Based Nanofluids-Hysteresis Phenomenon", *International Journal of Heat and Fluid Flow*, Vol. 28, No. 6, pp. 1492-1506.

Oh, D.-W., A. Jain, J. K. Eaton, K. E. Goodson, J. S. Lee, 2008, "Thermal Conductivity Measurement and Sedimentation Detection of Aluminum Oxide Nanofluids by Using the 3 Omega Method", *International Journal of Heat and Fluid Flow*, Vol. 29, No. 5, pp. 1456-1461.

Patel, H., T. Sundararajan, T. Pradeep, A. Dasgupta, N. Dasgupta, N., and S. K. Das, 2005, "A Micro-Convection Model for Thermal Conductivity of Nanofluids", *Pramana Journal of Physics*, Vol. 65, No. 5, pp. 863-869.

Perez-Maqueda, L. A., J. M. Blanes, J. Pascual, J. L. Perez-Rodriguez, 2004, "The Influence of Sonication on the Thermal Behavior of Muscovite and Biotite", *Journal of the European Ceramic Society*, Vol. 24, No. 9, pp. 2793-2801.

Prasher, R., P. Bhattacharya, P. E. Phelan, 2005, "Thermal Conductivity of Nanoscale Colloidal Solutions (Nanofluids)", *Physical Review Letters*, Vol. 94, No. 2.

Prasher, R., W. Evans, P. Meakin, J. Fish, P. Phelan, P. Keblinski, 2006, "Effect of Aggregation on Thermal Conduction in Colloidal Nanofluids" *Applied Physics Letters*, Vol. 89, No. 14.

Prasher, R., D. Song, J. Wang, and P. Phelan, 2006, "Measurements of Nanofluid Viscosity and Its Implications for Thermal Applications", *Applied Physics Letters*, Vol. 89, No. 13.

Shaikh, S., K. Lafdi, R. Ponnappan, 2007, "Thermal Conductivity Improvement in Carbon Nanoparticle Doped PAO Oil: An Experimental Study", *Journal of Applied Physics*, Vol. 101, No. 6.

Shima, P. D., J. Philip, B. Raj, 2009, "Role of Microconvection Induced by Brownian Motion of Nanoparticles in the Enhanced Thermal Conductivity of Stable Nanofluids", *Applied Physics Letters*, Vol. 94, No. 22.

Sleiti, A. K., 2011, "Rheological Characteristics of Boron Nitride Nanofluids with Polyalpha-Olein Oil Base Fluid", *Proceedings of IMECE 2011*, Denver, Colorado, USA.

Taha-Tijerina, J., T. N. Narayanan, G. Gao, M. Rohde, M., T. A. Tsentalovich, M. Pasquali, and P. M. Ajayan, 2012, "Electrically Insulating Thermal Nano-Oils Using 2D Fillers", *Acs Nano*, Vol. 6, No. 2, pp. 1214-1220.

Teng, T. P., Y. H. Hung, T. C: Teng, H. E. Mo, H. G. Hu, 2010, "The Effect of Alumina/Water Nanofluid Particle Size on Thermal Conductivity", *Applied Thermal Engineering*, Vol. 30, No. 14-15, pp. 2213-2218.

Timofeeva, E. V., A. N. Gavrilov, J. M. Mc Closkey, Y. V. Tolmachev, S. Sprunt, L. M. Lopatina, and J. V. Selinger, 2007, "Thermal Conductivity and Particle Agglomeration in Alumina Nanofluids: Experiment and Theory", *Physical Review E*, Vol. 76, No. 6.

Utomo, A. T., H. Poth, P. T. Robbins, and A. W. Pacek, 2012, "Experimental and Theoretical Studies of Thermal Conductivity, Viscosity and Heat Transfer Coefficient of Titania and Alumina Nanofluids", *International Journal of Heat and Mass Transfer*, Vol. 55, No. 25-26, pp. 7772-7781.

Venerus, D. C., J. Buongiorno, R. Christianson, J. Townsend, I. C. Bang, G. Chen, S. J. Chung, M. Chyu, H. Chen, Y. Ding, F. Dubois, G. Dzido, D. Funfschilling, Q. Galand, J. Gao, H. Hog, M. Horton, L. Hu, C. S. Iorio, A. B. Jarzebski, Y. Jiang, S. Kabelac, M. A. Kedzierski, C. Kim, T. McKrell, R. Ni, J. Phillip, N. Prabhat, P. Song, S. V. Vaerenbergh, D. Wen, S. Witharana, X.-Z. Zhao, S.-Q. Zhou, 2010, "Viscosity Measurements on Colloidal Dispersions (Nanofluids) for Heat Transfer Applications", *Applied Rheology*, Vol. 20, No. 4.

Wang, H. and M. Sen, 2009, "Analysis of the 3-Omega Method for Thermal Conductivity Measurement", *International Journal of Heat and Mass Transfer*, Vol. 52, No. 7-8, pp. 2102-2109.

Wang, X.-J., and X. F. Li, 2009, "Influence of pH on Nanofluids' Viscosity and Thermal Conductivity", *Chinese Physics Letters*, Vol. 26, No. 5.

Wang X, X. Xu, and S. U. S. Choi, 1999, "Thermal Conductivity of Nanoparticle-Fluid Mixture", *Journal of Thermophysical Heat Transfer*, Vol. 13, pp. 474–480.

Wang, X.-j., D.-s. Zhu, S. Yang, 2009, "Investigation of pH and SDBS on Enhancement of Thermal Conductivity in Nanofluids", *Chemical Physics Letters*, Vol. 470, No. 1-3, pp. 107-111.

Wei, X., H. Zhu, T. Kong, L. Wang, 2009, "Synthesis and Thermal Conductivity of Cu_2O Nanofluids", *International Journal of Heat and Mass Transfer*, Vol. 52, No. 19-20, pp. 4371-4374.

Wen, D. S. and Y. L. Ding, 2004, "Effective Thermal Conductivity of Aqueous Suspensions of Carbon Nanotubes (Carbon Nanotubes Nanofluids)", *Journal of Thermophysics and Heat Transfer*, Vol. 18, No. 4, pp. 481-485.

Witharana, S., C. Hodges, D. Xu, X. Lai, and Y. Ding, 2012, "Aggregation and Settling in Aqueous Polydisperse Alumina Nanoparticle Suspensions", *Journal of Nanoparticle Research*, Vol. 14, No. 5.

Wu, D. X., H. T. Zhu, L. Q. Wang, and L. M. Liu, 2009, "Critical No.s in Nanofluids Preparation, Characterization and Thermal Conductivity.", *Current Nanoscience*, Vol. 3, pp. 103-112.

Xie, H. Q., J. C. Wang, T. G. Xi, Y. Liu, F. Ai, Q. R. Wu, 2002, "Thermal Conductivity Enhancement of Suspensions Containing Nanosized Alumina Particles", *Journal of Applied Physics*, Vol. 91, No. 7, pp. 4568-4572.

Xuan, Y. M., and Q. Li, 2000, "Heat Transfer Enhancement of Nanofluids", *International Journal of Heat and Fluid Flow*, Vol. 21, No. 1, pp. 58-64.

Yang, J., Q. Jiang, 2010, "Preliminary Study on the Dynamic Stability of TiO_2-Water Based Nanofluids Flow in Circular Tube", *ASME 2009 2nd International Conference on Micro/Nanoscale Heat and Mass Transfer*, Shanghai, Peoples R China, December 18-21, 2009.

Yoo, D. H., K. S. Hong, H.-S. Yang, 2007, "Study of Thermal Conductivity of Nanofluids for the Application of Heat Transfer Fluids", *Thermochimica Acta*, Vol. 455, No. 1-2, pp. 66-69.

Yu, W. and S. U. S. Choi, 2003, "The Role of Interfacial Layers In the Enhanced Thermal Conductivity of Nanofluids: A Renovated Maxwell Model", *Journal of Nanoparticle Research*, Vol. 5, No. 1-2, pp. 167-171.

Zhi, C., Y. B. Xu, Y. Bando, D. Golberg, 2011, "Highly Thermo-Conductive Fluid with Boron Nitride Nanofillers", *Acs Nano*, Vol. 5, No. 8, pp. 6571-6577.

Zhu, D. S., X. F. Li, N. Wang, X. J. Wang, J. W. Gao, H. Li, 2009, "Dispersion Behavior and Thermal Conductivity Characteristics of Al_2O_3-H_2O Nanofluids", *Current Applied Physics*, Vol. 9, No. 1, pp. 131-139.

Zhu, H., C. Li, D. X. Wu, C. Y. Zhang, Y. S. Yin, 2010, "Preparation, Characterization, Viscosity and Thermal Conductivity of $CaCO_3$ Aqueous Nanofluids", *Science China-Technological Sciences*, Vol. 53, No. 2, pp. 360-368.

Zhu, H., C. Zhang, Y. M. Tang, J. X. Wang, B. Ren, Y. S. Yin, 2007, "Preparation and Thermal Conductivity of Suspensions of Graphite Nanoparticles", *Carbon*, Vol. 45, No. 1, pp. 226-228.